

Open quantum generalisation of Hopfield neural networks

P. Rotondo,^{1,2} M. Marcuzzi,^{1,2} J. P. Garrahan,^{1,2} I. Lesanovsky,^{1,2} and M. Müller³

¹*School of Physics and Astronomy, University of Nottingham, Nottingham, NG7 2RD, UK*

²*Centre for the Mathematics and Theoretical Physics of Quantum Non-equilibrium Systems, University of Nottingham, Nottingham NG7 2RD, UK*

³*Department of Physics, Swansea University, Singleton Park, Swansea SA2 8PP, UK*

We propose a new framework to understand how quantum effects may impact on the dynamics of neural networks. We implement the dynamics of neural networks in terms of Markovian open quantum systems, which allows us to treat thermal and quantum coherent effects on the same footing. In particular, we propose an open quantum generalisation of the celebrated Hopfield neural network, the simplest toy model of associative memory. We determine its phase diagram and show that quantum fluctuations give rise to a qualitatively new non-equilibrium phase. This novel phase is characterised by limit cycles corresponding to high-dimensional stationary manifolds that may be regarded as a generalisation of storage patterns to the quantum domain.

Introduction— Neural networks (NNs) [1] - artificial systems inspired by the neural structure of the brain - have become essential tools for solving tasks where more traditional rule-based algorithms fail. Examples are pattern and speech recognition [2], artificial intelligence [3, 4], and the analysis of big data [5]. All these NNs evolve according to the laws of classical physics.

It is widely believed that computational processes can benefit by exploiting the properties of quantum mechanics. Seminal works by Shor [6] and Grover [7] have proven the existence of quantum algorithms that systematically outperform their classical counterparts. More recently, we have seen the advent of a first generation of quantum information processors: for instance, Shor's algorithm for the factorization of integer numbers has been implemented on a trapped-ion quantum computer [8] and D-Wave machines, based on superconducting qubits, are envisioned to solve a particular class of NP-hard problems via quantum annealing [9–11].

An important and timely question is whether it is possible to take advantage of quantum effects in NN computing [12]. To date, however, none of the existing proposals [13–15] allows to define a satisfactory framework to consider quantum effects in NN dynamics. The problem is a conceptual one: the dynamics of closed quantum systems is governed by deterministic temporal evolution equations, whereas NNs are always described by dissipative dynamical equations, thus preventing any straightforward generalization of NNs computing in quantum systems [16]. Here we overcome this obstacle, by proposing a framework for quantum NNs based on open quantum systems (OQSs). We consider, in particular, the conceptually simplest case of Markovian dynamics, where the evolution of the density matrix is described by a Lindblad equation [17].

In order to make our ideas concrete we introduce a generalisation based on OQSs of one of the most studied NN systems, the Hopfield model [18] (see Fig. 1). The dissipative part of the dynamics corresponds to the thermal stochastic dynamics of the classical model (of-

ten realised via classical Monte Carlo dynamics), while quantum effects are due to a transverse field Hamiltonian that turns this classical equilibrium system into a quantum non-equilibrium one. In this approach, the result of a NN computation is imprinted on the long time density matrix, whose properties as a function of the control parameters (temperature, quantum driving, initial state) determine the phase diagram of the system. This setup reduces to the classical Hopfield NN when the quantum Hamiltonian is removed. By means of mean-field methods (which are exact for fully connected models such as this one) we calculate the phase diagram of the model, and show that a new non-equilibrium phase, characterized by the presence of limit cycles (LCs), arises due to the competition between coherent and dissipative dynamics. This may be regarded as a quantum generalisation of the retrieval phase of the classical Hopfield model.

Classical Hopfield NNs— Originally, the Hopfield NN was introduced as a toy model of *associative memory*. In the human brain memory patterns are stored and can be retrieved by association, i.e., when a pattern similar enough to one of those stored is presented to the NN the system is able to retrieve the correct one via classical annealing. The two fundamental ingredients to reproduce this are: (i) a dynamics on a system of N binary spins ($\sigma_i = \pm 1$, $i = 1, \dots, N$), that represent neuron activity (+1 firing and -1 silent); (ii) an appropriate prescription for the couplings J_{ij} that connect the i -th neuron with the j -th one, which must be able to store a set of p different memory patterns $\xi_i^{(\mu)}$ (i.e. fixed spin configurations) with $i = 1, \dots, N$, $\mu = 1, \dots, p$. In this language, *memory retrieval* denotes a phase in which the dynamics drives the system towards configurations which are closely resembling one of the $\xi_i^{(\mu)}$ for some μ . It turns out that the following discrete time dynamics fulfills these requirements:

$$\sigma_i(t+1) = \text{sign} \left(\sum_{j \neq i} J_{ij} \sigma_j(t) \right), \quad J_{ij} = \frac{1}{N} \sum_{\alpha=1}^p \xi_i^{(\alpha)} \xi_j^{(\alpha)}. \quad (1)$$

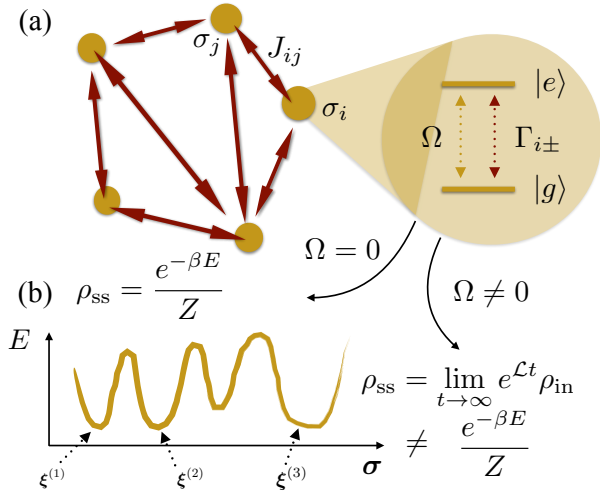


FIG. 1. (a) In the Hopfield model neurons (dots) are binary spins describing the activity of the neurons (+1 firing, -1 silent). The OQSs framework allows us to study the competition between thermal and quantum effects. In particular, the i -th neuron changes its activity state at a rate $\Gamma_{i\pm}$ as in the classical model or undergoes a quantum state change, due to the coherent driving introduced in Eq. (4). (b) If $\Omega = 0$, the stationary state is at thermal equilibrium. The qualitative behavior of the energy function of the classical NN is sketched in a one dimensional projection of the configurational space. Memory patterns are stored as the energy minima of the energy function. Whenever the NN is initialized close enough (close in the sense of the *Hamming distance* between spin configurations) to a specific memory pattern, the dynamics in Eq. (1) allows to retrieve the corresponding stored pattern. In the presence of quantum effects ($\Omega \neq 0$), the nature of the stationary state can be non-trivial, i.e. it may be non-thermal, due to the competition between quantum coherence and irreversible classical dynamics.

Eq. (1) describes a zero temperature Monte Carlo dynamics that can be easily generalized to include thermal effects [19]. Moreover it can be proven that this dynamics minimizes the energy function $E = -\frac{1}{2} \sum_{i \neq j} J_{ij} \sigma_i \sigma_j$, namely an Ising model with pattern-dependent couplings. Techniques used in the statistical physics of disordered systems enable to investigate Hopfield NNs (and more general types of NNs) quantitatively [19–21]. In statistical physics language, the retrieval phase is the low temperature phase corresponding to an energy landscape where memory patterns are stable states of the NN, i.e. the thermal equilibrium stationary states; see Fig. 1.

Open quantum Hopfield NNs—To introduce quantum effects, we employ a description of the NN dynamics in terms of open quantum master equations. The starting point of our analysis is a master equation in Lindblad form for the density matrix ρ :

$$\dot{\rho} = -i[H, \rho] + \sum_{i=1}^N \sum_{\tau=\pm} \left(L_{i\tau} \rho L_{i\tau}^\dagger - \frac{1}{2} \{L_{i\tau}^\dagger L_{i\tau}, \rho\} \right), \quad (2)$$

where we define a set of jump operators as follows:

$$L_{i\pm} = \Gamma_{i\pm} \sigma_i^\pm, \quad \Gamma_{i\pm} = \frac{e^{\mp \beta/2 \Delta E_i}}{(2 \cosh(\beta \Delta E_i))^{\frac{1}{2}}}. \quad (3)$$

Here $\beta = 1/T$ is the inverse temperature, $\Delta E_i = \sum_{j \neq i} J_{ij} \sigma_j^z$ the change in energy under flipping of the i -th spin, and $\sigma_i^\pm = (\sigma_i^x \pm i \sigma_i^y)/2$, with $\sigma^{x,y,z}$ the Pauli matrices. Quantum effects are included by a uniform transverse field in the x -direction, corresponding to a Hamiltonian,

$$H = \Omega \sum_{i=1}^N \sigma_i^x. \quad (4)$$

In the absence of this term, Eq. (2) describes a classical stochastic dynamics: any initial density matrix that is diagonal in the σ^z basis remains diagonal under the evolution and Eq. (2) reduces to $\dot{P} = \sum_{i=1}^N \sum_{\tau=\pm} \Gamma_{i\tau}^2 \left[\sigma_i^\tau - \frac{1}{2} (1 + \tau \sigma_i^z) \right] P$, where P is the probability vector formed by the diagonal of ρ . The rates $\Gamma_{i\tau}^2$ obey detailed balance with respect to the Boltzmann distribution for energy E at temperature T , so that this is the master equation for the classical Hopfield NN, as shown in the supplementary material (SM) [22].

Mean-field solution— Since the NN is defined in terms of fully-connected interactions, the mean-field approximation should be exact [22]. We consider the equations of motion for the time-dependent operators σ_i^z , σ_i^\pm . These $3N$ equations can be reduced to a closed set of equations for the $2p$ collective operators $s_\mu^\alpha = (1/N) \sum_{i=1}^N \xi_i^{(\mu)} \sigma_i^\alpha$ ($\alpha = z, y$). The mean-field approximation considers the evolution of the averaged collective variables $m_\mu^{z,y} = \langle s_\mu^{z,y} \rangle$ neglecting correlations between them [22]. The evolution equations then read:

$$\dot{\mathbf{m}}^z = 2\Omega \mathbf{m}^y + \frac{1}{N} \sum_{i=1}^N \xi_i \tanh(\beta \xi_i \cdot \mathbf{m}^z) - \mathbf{m}^z, \quad (5)$$

$$\dot{\mathbf{m}}^y = -2\Omega \mathbf{m}^z - \frac{1}{2} \mathbf{m}^y, \quad (6)$$

where we introduced a vectorial notation for both the collective operators and the memory patterns, $\mathbf{m}^\alpha = (m_1^\alpha, \dots, m_p^\alpha)$. m_μ^z represents the overlap between the μ -th memory pattern and the neuronal configuration of the system (in the z direction), and thus can be used as an *order parameter*: if in the stationary state $m_1^z \approx (1, 0, \dots, 0)$, this means that the NN correctly retrieved the first pattern stored (and similarly for the other $p-1$ patterns). Setting $\dot{\mathbf{m}}^z = \dot{\mathbf{m}}^y = \mathbf{0}$ in Eqs. (5,6) we get the equations for the stationary solutions:

$$(1 + 8\Omega^2) \mathbf{m}^z = \overline{\xi \tanh(\beta \xi \cdot \mathbf{m}^z)}, \quad (7)$$

where we have assumed *self-averaging*, typical of disordered systems [23] in the large N limit, i.e., $1/N \sum_{i=1}^N f(\xi_i) \rightarrow \overline{f(\xi)}$, where $\overline{(\cdot)}$ is the average over

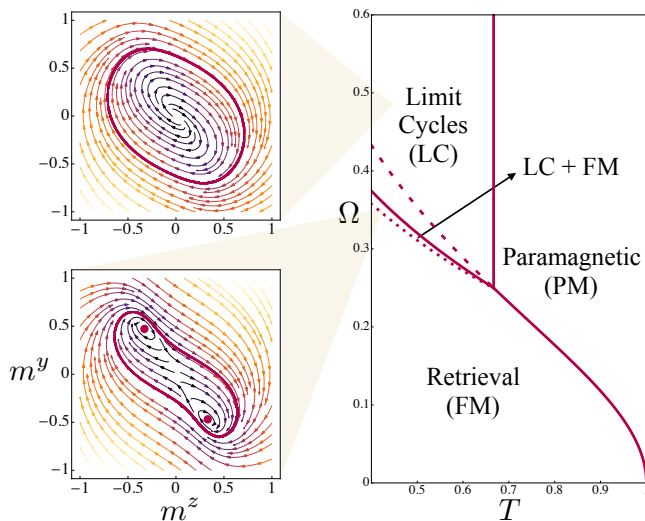


FIG. 2. Phase diagram of the OQS generalization of the Hopfield model in the (T, Ω) plane. The NN displays a paramagnetic phase in the high temperature regime, with a stable attractor in $\mathbf{m}^z = \mathbf{0}$. The boundary of the paramagnetic phase is established by looking at the stability of this attractor. In the low T and Ω regime the system is in the ferromagnetic (retrieval) phase, whereas for low T but sufficiently large Ω , the NN displays a LC (top left), which is the only stable attractor once the ferromagnetic solutions become unstable. However the LC appears well below this line (and above the dotted line), producing a small region of phase coexistence (see flux diagram at bottom left). Above the dashed line and for $T < 2/3$, the ferromagnetic solutions disappear.

the disorder distribution. Equations (5,6) allow to study the interplay between the retrieval and the paramagnetic phases of the NN. It is worth remarking, however, that a more general approach, involving the replica method, is required to deal with the spin glass phase arising when an extensive number of memory patterns is loaded into the NN [20]. In the following we focus on the retrieval phase of our OQS, which amounts to considering the case of a finite number of patterns p .

As a first step, we notice that Eq. (7) has the same form of the mean-field equation obtained for the classical Hopfield NN [19]: in particular a suitable rescaling of \mathbf{m}^z with an effective temperature $T_{\text{eff}} = T(1 + 8\Omega^2)$ establishes their equivalence. This means that the structure of the stationary points of the dynamics is equivalent to the classical one up to a rescaling of the temperature. In particular, the retrieval solutions $\mathbf{m}^z \approx (1, \dots, 0)$, the paramagnetic solution $\mathbf{m}^z = \mathbf{0}$, as well as the whole set of metastable states (spurious memories) [19] are still fixed points of the quantum dynamics. Closer inspection of Eqs. (5,6) reveals, however, that quantum driving does more than just rescale temperature.

Beyond these stationary solutions, the mean-field equations (5,6) also display time-dependent periodic solutions at long times. A simple way to gain insight on

this new feature is to consider a high- T expansion of Eqs. (5,6) up to the first non-linear order. In this case the equations become analogous to a Lotka-Volterra (LV) dynamical system, widely studied in the literature on ecological systems [24]. Under appropriate conditions, a LV system is known to have limit cycles (LCs) solutions.

The observation above suggests that our open quantum Hopfield NN can feature at least three possible phases in the (T, Ω) plane: (i) a paramagnetic phase where the dynamics converges to the trivial solution $\mathbf{m}^z = \mathbf{0}$; (ii) a retrieval phase where the attractor of the system is one of the non-trivial solutions of Eq. (7); (iii) a novel time-dependent stationary phase, emerging from the competition between the dissipative and coherent dynamics.

Phase diagram— To characterize the phase diagram of this OQS in the (T, Ω) plane, we follow two different routes: (i) we solve numerically the mean-field equations at low p by averaging over disorder using the factorized probability distribution $P(\xi) = \prod_{\alpha=1}^p p(\xi^{(\alpha)})$ with $p(\xi) = 1/2\delta(\xi - 1) + 1/2\delta(\xi + 1)$; (ii) we perform a *Lyapunov linear stability analysis* [25], namely we study the dynamical stability of the stationary points under small perturbations (see [22] for details). Through either approach we identify the boundaries of the different phases.

The phase diagram of the NN is summarized in Fig. 2. For $T > 2/3$ and $\Omega > \sqrt{(1-T)/8T}$ the system is in the paramagnetic phase. Retrieval is possible in the low temperature and low Ω regime, whereas the dynamics features LCs as a stationary manifold in the low temperature and high coherence regime. At the boundary between the retrieval and the LC phase, we recognize a small region where the two phases coexist: initializing the system close enough to $(\mathbf{m}^z, \mathbf{m}^y) = (\mathbf{0}, \mathbf{0})$, drives the NN towards the retrieval solutions, whereas initial conditions chosen outside a critical hypervolume centered around $(\mathbf{0}, \mathbf{0})$ converge to the LC (see insets in Fig 2).

For a single pattern, $p = 1$, we are able to rigorously prove the presence of a LC phase, since Eqs. (5) and (6) can be recast in *Liénard form* [26], (see also [22]) for $T < 2/3$ and $T > (8\Omega^2 + 1)^{-1}$. The Liénard theorem [27] guarantees the existence, uniqueness and stability of a LC (which wraps around the origin).

The LC phase can be interpreted as a new quantum retrieval phase: for low enough temperatures, in fact, independently from the initial conditions the NN is always driven towards a LC with a large oscillation amplitude. For instance, the case reported in Fig. 3a (corresponding to $T = 0.15$) shows oscillations reaching a maximum overlap of ~ 0.8 with the single stored pattern. Limit cycles of this kind (involving mostly a single overlap) also exist for generic $p > 1$. Numerical evidence suggests that at long times oscillations involve at most two overlaps, while all the remaining $p - 2$ asymptotically vanish. More importantly, when starting from an initial condition with large overlap with one of the patterns (say, the μ -th one) and significantly smaller overlap with the remaining ones

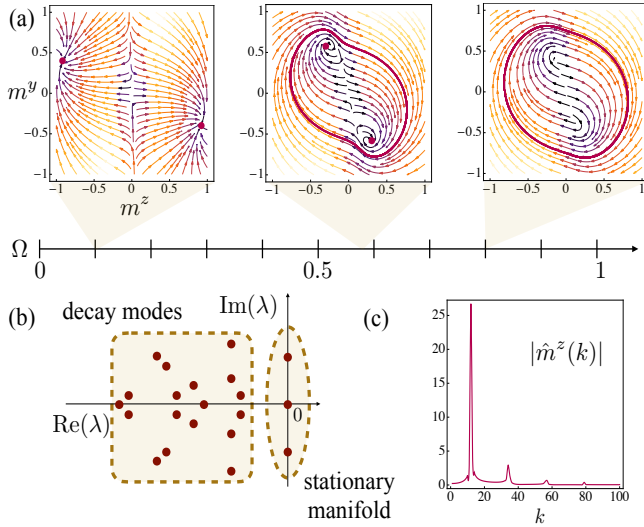


FIG. 3. (a) From left to right flux diagrams of the mean-field dynamics at $T = 0.15, \Omega = 0.1, 0.58, 0.8$. The different attractors are highlighted in each panel. In the bulk of the LC phase the maximum overlap with one of the stored patterns is ~ 0.8 , independently from the initial conditions, suggesting that also this phase can be interpreted as a retrieval phase. (b) Sketch of the spectrum of a plausible Liouvillian super-operator describing the LC shown in (a). Time-dependent periodic stationary states require at least a conjugate pair of purely imaginary eigenvalues. (c) The structure of the Fourier components $|\hat{m}^z(k)|$ of the top right LC, justifies the single frequency approximation made in the main text.

seems to always lead to oscillations in the (m_μ^z, m_μ^y) plane and vanishing ones in the others. This hints at the possibility of associating to any stable fixed point attractor $\xi_i^{(\mu)}$ of the NN a corresponding LC attractor. It is moreover noteworthy that the fundamental properties of the Hopfield dynamics are rather robust against the introduction of a coherent term such as the transverse field we use in this work. It is worth remarking that this robustness is closely related to symmetry arguments: indeed the generalized Z_2 symmetry broken in the FM phase of the classical model is still broken in the LC phase. Here, additionally, the stationary state spontaneously breaks the time translation symmetry, which should correspond to the appearance of a Goldstone mode, as found in [28].

Quantum nature of the LC phase— Examples of LC phases in classical Hopfield NNs with asymmetric couplings exist [29, 30]. However, the LC phase that we find here is intimately related to the competition between coherent and dissipative dynamics. The persistence of oscillations in the long time limit implies the survival – to a degree – of quantum coherence. To substantiate this claim, we argue in the following what the structure of the *stationary manifold* of the Lindblad equation should be, following the classification of Refs. [31–33] for the case of systems with finite-dimensional Hilbert spaces.

By formally integrating Eq. (2) we get $\rho(t) = e^{t\mathcal{L}}\rho_{\text{in}}$,

where \mathcal{L} is the generator of the open quantum dynamics [i.e., $\mathcal{L}\rho$ is shorthand for the r.h.s. of Eq. (2)], and ρ_{in} is the initial state. Assuming \mathcal{L} to be diagonalizable, the density matrix can be further expanded as [34]:

$$\rho(t) = \sum_{l=1}^{2^N} c_l e^{t\lambda_l} R_l, \quad (8)$$

where λ_l are the eigenvalues, R_l are the right eigenmatrices of \mathcal{L} , i.e. $\mathcal{L}R_l = \lambda_l R_l$, and c_l the components of the initial state on these eigenmodes. Because of preservation of probability and positivity, the eigenvalues of \mathcal{L} have non-positive real parts and are either real or come in complex conjugate pairs. The stationary manifold is constructed from all the R_l for which $\text{Re}(\lambda_l) = 0$; we define n its dimension and reorder the eigenvalues such that the zero ones appear first. If $\lambda_l = 0 \forall l = 1, \dots, n$ then each initial state maps to a state in the stationary manifold asymptotically and no time dependence survives at long times. To allow for limit cycles, \mathcal{L} must display at least a pair of conjugate, purely-imaginary eigenvalues $\pm i\omega$, as sketched in Fig. 3b. The long time evolution due to the presence of these eigenvalues is unitary and one could formally define a corresponding reduced Hamiltonian acting coherently on the stationary subspace [33–35].

A Fourier analysis of the LCs (see Fig 3c) justifies a single frequency approximation for the stationary state, leading to $\rho_{\text{ss}}(t) \sim R_0 + R_1 + R_2 e^{i\omega t} + R_2^\dagger e^{-i\omega t}$, that allows to obtain a quantitative agreement with the numerics by requiring that the R_i 's are such that: $\text{Tr}(s^\alpha R_{0/1}) = 0$, $\text{Tr}(s^z R_2) = \bar{m}^z$ and $\text{Tr}(s^y R_2) = \bar{m}^y e^{i\epsilon}$. This choice reproduces a LC in the (m^z, m^y) plane parameterized as $m^z(t) = \text{Tr}(s^z \rho_{\text{ss}}(t)) \sim \bar{m}^z \cos(\omega t)$ and $m^y(t) = \text{Tr}(s^y \rho_{\text{ss}}(t)) \sim \bar{m}^y \cos(\omega t + \epsilon)$ (with ϵ a proper real phase).

Summary and Outlook— We proposed a framework based on open quantum systems to investigate quantum effects in the dynamics of neural networks. We applied this approach to an open system quantum generalization of the celebrated Hopfield model. As in the classical case it is possible to use a mean-field treatment to determine the phase diagram. We identified a retrieval phase with fixed points associated to classical patterns and quantum effects can be accounted for by an effective temperature. We moreover found a novel phase characterized by limit cycles which are a consequence of the quantum driving. Our approach is a natural extension of the NN paradigm into the domain of open quantum systems. It shows that the resulting phase structure of such systems can indeed be richer than that of their classical counterparts. Future investigations are needed in order to clarify whether practical applications of NNs can benefit from quantum effects, similar to their rule-based counterparts, the classical computers.

The research leading to these results has received funding from the European Research Council un-

der the European Union's Seventh Framework Programme (FP/2007-2013) / ERC Grant Agreement No.

335266 (ESCQUMA), the H2020-FETPROACT-2014 Grant No.640378 (RYSQ), and EPSRC Grant No. EP/M014266/1.

Supplemental Material to “Open quantum generalisation of Hopfield neural networks”

CONTENTS

Basic definitions	1
Derivation of the mean field equations for the open quantum Hopfield NN	2
Classical limit of the quantum master equation	2
Addition of a quantum term	3
Dynamical mean field equations and stationary state equations	6
Mapping out the phase diagram: stability analysis of the stationary state solutions	7
Stability analysis of the paramagnetic solution	7
Appearance and stability of the ferromagnetic solutions	9
Role of the effective temperature	10
Limit cycle phase: exact results and numerical solution	11
Representation of the $p = 1$ case in terms of a Liénard equation	11
Representation of the $p = 1$ case in terms of a single $N/2$ -spin	12
The 2-memories case	12
Decoupling of the equations in the 2-memories case	13
The 3-memories case	14
Bounds to the appearance of limit cycles	16
References	18

BASIC DEFINITIONS

The Hopfield model [18] is a stochastic process with rates engineered to satisfy detailed balance with energy function

$$E = -\frac{1}{2N} \sum_{\mu=1}^p \sum_{i,j=1}^N \xi_i^{(\mu)} \xi_j^{(\mu)} \sigma_i \sigma_j = -\frac{1}{2N} \sum_{\mu=1}^p \left(\sum_{i=1}^N \xi_i^{(\mu)} \sigma_i \right)^2, \quad (\text{S1})$$

where N is the number of spin variables (or lattice sites) in the system and p the number of patterns (memories) one is trying to store in the network. Each of these memories is encoded in terms of an N -dimensional vector $\xi^{(\mu)}$, whose components are independent, identically-distributed random variables, and are usually taken to be classical Ising spins which assume the values ± 1 with equal probability. For later convenience, we define the coupling matrix and the overlap of the spin configuration σ with the μ -th memory pattern as

$$J_{ij} = \frac{1}{N} \sum_{\mu=1}^p \xi_i^{(\mu)} \xi_j^{(\mu)}, \quad m_\mu = \frac{1}{N} \sum_{i=1}^N \xi_i^{(\mu)} \sigma_i, \quad (\text{S2})$$

respectively. This makes it possible to re-express the energy as

$$E = -\frac{N}{2} \sum_{\mu=1}^p m_\mu^2. \quad (\text{S3})$$

In the absence of metastable minima, the perfect retrieval of one of the stored patterns can be achieved via a proper zero-temperature Monte Carlo dynamics, e.g., with discrete updates

$$\sigma_i(t+1) = \text{sign}(\Delta E_i(t)), \quad \Delta E_i(t) = \sum_{j \neq i} J_{ij} \sigma_j(t), \quad (\text{S4})$$

on the system configuration, where $\Delta E_i(t)$ is the energy difference due to a single spin-flip of σ_i at step t . As mentioned above, this dynamics can be easily generalized to include thermal fluctuations at a fixed temperature $T = 1/\beta$. In this case, the probability of performing a single Monte Carlo update $\sigma_i(t) \rightarrow \sigma_i(t+1)$ is given by

$$P(\sigma_i(t+1)) = \frac{e^{\beta(\sigma_i(t+1)\Delta E_i(t))}}{2 \cosh(\beta \sigma_i(t+1) \Delta E_i(t))}. \quad (\text{S5})$$

DERIVATION OF THE MEAN FIELD EQUATIONS FOR THE OPEN QUANTUM HOPFIELD NN

A first step towards the inclusion of quantum effects in the Hopfield neural network is to reformulate the classical dynamics as a purely dissipative quantum master equation. For Markovian evolution, the density matrix of the system ρ evolves under the Lindblad equation

$$\dot{\rho} = \mathcal{L}\rho, \quad \mathcal{L} = \sum_k L_k(\cdot) L_k^\dagger - \frac{1}{2} \{L_k^\dagger L_k, (\cdot)\}, \quad (\text{S6})$$

with \mathcal{L} the superoperator, L_k the Linblad jump operators labeled by an index k and $\{A, B\} = AB + BA$ denoting anticommutation. A possible strategy to reproduce the classical dynamics of the Hopfield model is to construct the jump operators in such a way that they generate the same local processes of the aforementioned heat-bath dynamics. More specifically, if we generalize our classical spins to quantum ones $\uparrow \rightarrow |\uparrow\rangle = (1, 0)^\top$, $\downarrow \rightarrow |\downarrow\rangle = (0, 1)^\top$, we can set

$$L_{i\pm} = \sqrt{\gamma} \frac{e^{\pm \beta \Delta E_i/2}}{(2 \cosh(\beta \Delta E_i))^{\frac{1}{2}}} \sigma_i^\pm \quad \text{with} \quad \Delta E_i = \sum_{j \neq i} J_{ij} \sigma_j^z \quad (\text{S7})$$

where γ is an overall amplitude determining the frequency of the jumps and σ_i^\pm and σ_i^z are the Pauli matrices acting on the i -th spin which, in the representation chosen above, read

$$\sigma^z = \begin{pmatrix} 1 & 0 \\ 0 & -1 \end{pmatrix}, \quad \sigma^+ = \begin{pmatrix} 0 & 1 \\ 0 & 0 \end{pmatrix}, \quad \sigma^- = (\sigma^+)^\top, \quad (\text{S8})$$

and satisfy the standard (anti-)commutation relations:

$$[\sigma_i^z, \sigma_j^\pm] = \pm 2\sigma_i^\pm \delta_{ij}, \quad [\sigma_i^+, \sigma_j^-] = \sigma_i^z \delta_{ij}, \quad \{\sigma_i^\pm, \sigma_i^z\} = 0, \quad \{\sigma_i^+, \sigma_i^-\} = \mathbb{1}_i. \quad (\text{S9})$$

The dynamics generated by Eq. (S6) features a special symmetry: working in the eigenbasis of the σ_i^z s (i.e., on states of the form $|\uparrow\uparrow\downarrow\dots\rangle$), if we express the generic matrix element $\rho_{ab} = \langle a|\rho|b\rangle$ and define $\mathcal{S}_h = \{\rho_{ab} : b - a = h\}$ one can check that the evolution equations for the matrix elements close within each subspace \mathcal{S}_h . Therefore, if one starts in the classical subspace $\mathcal{S}_0 = \{|a\rangle\langle a|\}$ the dynamics remains confined within it and no overlap over non-classical states is generated in time. Therefore, the dynamics is exactly reduced to a stochastic process over the probabilities p_a of the “configurations” $|a\rangle\langle a|$; below we show that this reconstructs a continuous-time variant of the heat-bath process described above.

Classical limit of the quantum master equation

For simplicity, we are going to analyze the evolution of observables, instead of states. By our discussion above, we can safely restrict ourselves to the identity and the σ_i^z s. The former does not evolve, while the latter obey the adjoint Lindblad equation

$$\dot{O} = \sum_k L_k^\dagger O L_k - \frac{1}{2} \{L_k^\dagger L_k, O\}, \quad (\text{S10})$$

which, once specialized to the case of interest, reads

$$\dot{\sigma}_i^z = \sum_{l,s} L_{ls}^\dagger \sigma_i^z L_{ls} - \frac{1}{2} \{L_{ls}^\dagger L_{ls}, \sigma_i^z\} \quad (\text{S11})$$

with $s = \pm$.

Remark: the Lindblad operators $L_{i\sigma}$ have the following form:

$$L_{i\pm} = \sqrt{\gamma} \Gamma_{i\pm} \sigma_i^\pm, \quad \Gamma_{i\pm} = \frac{e^{\pm\beta/2\Delta E_i}}{(2 \cosh(\beta\Delta E_i))^{\frac{1}{2}}}, \quad \Delta E_i(\sigma_1^z, \dots, \sigma_N^z) = \sum_{j \neq i} J_{ij} \sigma_j^z \quad (\text{S12})$$

implying that $\Gamma_{i\pm}$ trivially acts as the identity on the i -th subspace and hence $[\Gamma_{i\pm}, \sigma_i^\pm] = 0$. Furthermore, since the Γ s are entirely defined in terms of the σ_i^z s, we have $[\Gamma_{i\pm}, \sigma_j^z] = 0 \ \forall i, j$. This allows us to rearrange terms in the Lindblad equation to get, for the “flipping-up” (+) process,

$$\begin{aligned} \mathcal{L}_+ \sigma_i^z &= \sum_{l=1}^N L_{l+}^\dagger \sigma_i^z L_{l+} - \frac{1}{2} \{L_{l+}^\dagger L_{l+}, \sigma_i^z\} = \gamma \sum_l \Gamma_{l+}^2 \left[\sigma_l^- \sigma_i^z \sigma_l^+ - \frac{1}{2} \{\sigma_l^- \sigma_l^+, \sigma_i^z\} \right] = \\ &= \gamma \Gamma_{i+}^2 \left[\sigma_i^- \sigma_i^z \sigma_i^+ - \frac{1}{2} \{\sigma_i^- \sigma_i^+, \sigma_i^z\} \right] + \underbrace{\gamma \sum_{l \neq i} \Gamma_{l+}^2 \left[\sigma_l^- \sigma_i^z \sigma_l^+ - \frac{1}{2} \{\sigma_l^- \sigma_l^+, \sigma_i^z\} \right]}_{=0}, \end{aligned} \quad (\text{S13})$$

where we used the fact that $[\sigma_l^\pm, \sigma_i^z] = 0$ for $i \neq l$. The only term remaining can be thus recast as

$$\mathcal{L}_+ \sigma_i^z = \gamma (1 - \sigma_i^z) \Gamma_{i+}^2. \quad (\text{S14})$$

Following an analogous procedure, one can calculate

$$\mathcal{L}_- \sigma_i^z = -\gamma (1 + \sigma_i^z) \Gamma_{i-}^2. \quad (\text{S15})$$

Adding these terms we get the evolution equation for σ_i^z :

$$\dot{\sigma}_i^z = \gamma \left[(1 - \sigma_i^z) \Gamma_{i+}^2 - (1 + \sigma_i^z) \Gamma_{i-}^2 \right] = -\gamma \sigma_i^z + \gamma \tanh(\beta \Delta E_i), \quad (\text{S16})$$

where for the last equality we have employed the identities

$$\Gamma_{i+}^2 + \Gamma_{i-}^2 = 1 \quad \text{and} \quad \Gamma_{i+}^2 - \Gamma_{i-}^2 = \tanh(\beta \Delta E_i) \quad (\text{S17})$$

Employing a mean field approximation and looking for the stationary properties (i.e., setting $\dot{\sigma}_i^z = 0$) of the system, the equations above yield the naive mean field equations of the Hopfield model (exact in the retrieval phase):

$$z_i = \tanh \left(\sum_{j \neq i} J_{ij} z_j \right), \quad (\text{S18})$$

with $z_i = \langle \sigma_i^z \rangle$.

Addition of a quantum term

The action of an Hamiltonian inducing a coherent evolution is accounted for by completing the Lindblad equation with a commutator:

$$\begin{aligned} \dot{\rho} &= -i[H, \rho] + \sum_k L_k \rho L_k^\dagger - \frac{1}{2} \{L_k^\dagger L_k, \rho\}, \\ \dot{O} &= i[H, O] + \sum_k L_k^\dagger O L_k - \frac{1}{2} \{L_k^\dagger L_k, O\}. \end{aligned} \quad (\text{S19})$$

We choose a coherent term of the form $H = \Omega \sum_{i=1}^N \sigma_i^x$ which couples classical and non-classical states. The equation of motion for σ_i^z acquires a new term

$$\dot{\sigma}_i^z = 2\Omega \sigma_i^y - \gamma \sigma_i^z + \gamma \tanh(\beta \Delta E_i), \quad (\text{S20})$$

which in the absence of dissipation ($\gamma = 0$) would simply describe Rabi oscillations of frequency 2Ω about the x axis. This clearly shows that the decoupling of the classical subspace does not hold any more: in fact, the equations for σ_z^i do not close and we need to write additional ones for $\sigma_i^{x/y}$ or, equivalently, σ_i^\pm . These are generically more involved, since these operators do not commute with the Γ s. To simplify the respective Lindblad equations, we will make use in the following of the anticommutation relations, which in particular imply that

$$f(\sigma_1^z, \dots, \sigma_j^z, \dots, \sigma_N^z) \sigma_j^\pm = \sigma_j^\pm f(\sigma_1^z, \dots, -\sigma_j^z, \dots, \sigma_N^z), \quad (\text{S21})$$

for any function f with a power series representation. Let us consider the equation for σ_i^+ :

$$\dot{\sigma}_i^+ = -i\Omega\sigma_i^z + \gamma \sum_l \sigma_l^- \Gamma_{l+} \sigma_i^+ \Gamma_{l+} \sigma_l^+ - \frac{1}{2} \{ \sigma_l^- \Gamma_{l+} \Gamma_{l+} \sigma_l^+, \sigma_i^+ \} + (+ \leftrightarrow -). \quad (\text{S22})$$

Our aim is now to move all the Γ 's to the right. This is done applying property (S21). Introducing the notation

$$\Gamma_{ls}^{(i)} = \Gamma_{ls}(\sigma_1^z, \dots, -\sigma_i^z, \dots, \sigma_N^z). \quad (\text{S23})$$

equation (S22) can be written in a compact form as

$$\begin{aligned} \dot{\sigma}_i^+ = & -i\Omega\sigma_i^z - \frac{\gamma}{2}\sigma_i^+(\Gamma_{i+}^2 + \Gamma_{i-}^2) + \frac{\gamma}{2}\sigma_i^+ \sum_{l \neq i} (1 - \sigma_l^z) \left(\Gamma_{l+}^{(i)} \Gamma_{l+} - \frac{1}{2} \Gamma_{l+}^{(i)} \Gamma_{l+}^{(i)} - \frac{1}{2} \Gamma_{l+} \Gamma_{l+} \right) + \\ & + \frac{\gamma}{2}\sigma_i^+ \sum_{l \neq i} (1 + \sigma_l^z) \left(\Gamma_{l-}^{(i)} \Gamma_{l-} - \frac{1}{2} \Gamma_{l-}^{(i)} \Gamma_{l-}^{(i)} - \frac{1}{2} \Gamma_{l-} \Gamma_{l-} \right). \end{aligned} \quad (\text{S24})$$

The equation for σ_i^- is simply obtained via hermitian conjugation of the one above. These equations can be simplified recognizing that Γ and $\Gamma^{(i)}$ depend on two configurations which differ by a single spin (the i -th one). It could be thereby reasonably expected that $\Gamma \approx \Gamma^{(i)}$ up to finite-size corrections which scale as $1/N$. More precisely, singling out the dependence on the i -th spin $\Gamma_{l\pm}(\sigma_1^z, \sigma_2^z, \dots, \sigma_N^z) \equiv F_{li\pm}(\beta J_{li} \sigma_i^z)$ (with no sum over repeated indices) we can generically write $F_{li\pm}(\beta J_{li} \sigma_i^z) = E_{li\pm} + O_{li\pm} \sigma_i^z$ with

$$E_{li\pm} = \frac{F_{li\pm}(\beta J_{li}) + F_{li\pm}(-\beta J_{li})}{2} \quad (\text{S25})$$

$$O_{li\pm} = \frac{F_{li\pm}(\beta J_{li}) - F_{li\pm}(-\beta J_{li})}{2} \quad (\text{S26})$$

the even and odd parts of $F_{li\pm}$ calculated in βJ_{li} . This can be understood by expanding $F_{li\pm}$ as a power series in σ_i^z and then grouping odd powers in O and even ones in E exploiting the well-known property

$$(\sigma_i^z)^n = \begin{cases} 1 & (n \text{ even}) \\ \sigma_i^z & (n \text{ odd}), \end{cases} \quad (\text{S27})$$

provided that the series expansion has a radius of convergence $\geq |\beta J_{li}|$, or otherwise taking the analytic continuation up to $\pm\beta J_{li}$. Clearly, $\Gamma_{l\pm}^{(i)} = F_{li\pm}(-\beta J_{li} \sigma_i^z)$ and we can write

$$\Gamma_{l\pm}^{(i)} = \Gamma_{l\pm}(g_{li\pm} + f_{li\pm} \sigma_i^z) \quad (\text{S28})$$

with

$$g_{li\pm} = \frac{E_{li\pm}^2 + O_{li\pm}^2}{E_{li\pm}^2 - O_{li\pm}^2} \quad \text{and} \quad f_{li\pm} = -\frac{2E_{li\pm}O_{li\pm}}{E_{li\pm}^2 - O_{li\pm}^2}. \quad (\text{S29})$$

Defining $\Delta E_{li} = \sum_{j \neq i, l} J_{lj} \sigma_j^z$ we can write $F_{li\pm}$ as

$$F_{li\pm}(+\beta J_{li}) = \frac{e^{\pm \frac{\beta}{2} (\Delta E_{li} + J_{li})}}{\sqrt{2 \cosh \beta (\Delta E_{li} + J_{li})}} \quad \text{and} \quad F_{li\pm}(-\beta J_{li}) = \frac{e^{\pm \frac{\beta}{2} (\Delta E_{li} - J_{li})}}{\sqrt{2 \cosh \beta (\Delta E_{li} - J_{li})}} \quad (\text{S30})$$

and consequently

$$g_{li\pm} = \frac{1}{2} \left\{ e^{\mp \beta J_{li}} \sqrt{\frac{\cosh \beta (\Delta E_{li} + J_{li})}{\cosh \beta (\Delta E_{li} - J_{li})}} + e^{\pm \beta J_{li}} \sqrt{\frac{\cosh \beta (\Delta E_{li} - J_{li})}{\cosh \beta (\Delta E_{li} + J_{li})}} \right\}, \quad (\text{S31})$$

$$f_{li\pm} = \frac{1}{2} \left\{ e^{\mp \beta J_{li}} \sqrt{\frac{\cosh \beta (\Delta E_{li} + J_{li})}{\cosh \beta (\Delta E_{li} - J_{li})}} - e^{\pm \beta J_{li}} \sqrt{\frac{\cosh \beta (\Delta E_{li} - J_{li})}{\cosh \beta (\Delta E_{li} + J_{li})}} \right\}. \quad (\text{S32})$$

Now, according to the definition (S2),

$$J_{li} = \frac{1}{N} \sum_{\mu} \xi_l^{(\mu)} \xi_i^{(\mu)}; \quad (\text{S33})$$

since $\xi_l^{(\mu)} \xi_i^{(\mu)}$ for $l \neq i$ are independent random variables which take the values ± 1 with equal probability, as long as p is large we can apply the central limit theorem to argue that $J_{li} \sim \sqrt{p}/N$. If p is kept fixed, or taken to scale slower than N^2 these contributions will hence vanish in the thermodynamic limit and only yield small corrections at finite – albeit large – size. We can thus perform a power series expansion

$$g_{li\pm} = g_{li\pm}^{(0)} + \beta J_{li} g_{li\pm}^{(1)} + (\beta J_{li})^2 g_{li\pm}^{(2)} + \dots \quad (\text{S34})$$

$$f_{li\pm} = f_{li\pm}^{(0)} + \beta J_{li} f_{li\pm}^{(1)} + (\beta J_{li})^2 f_{li\pm}^{(2)} + \dots, \quad (\text{S35})$$

where summation on repeated indices is *not* intended. The first few terms read

$$\begin{aligned} g_{li\pm}^{(0)} &= 1 & f_{li\pm}^{(0)} &= 0 \\ g_{li\pm}^{(1)} &= 0 & f_{li\pm}^{(1)} &= \mp 1 + \tanh \beta \Delta E_{li} \\ g_{li\pm}^{(2)} &= \frac{1}{2} (1 \mp \tanh \beta \Delta E_{li})^2 & f_{li\pm}^{(2)} &= 0. \end{aligned} \quad (\text{S36})$$

Stopping at first order, we find

$$\begin{aligned} \Gamma_{l\pm}^{(i)} &= \Gamma_{l\pm} \left[1 + \beta J_{li} (\mp 1 + \tanh (\beta \Delta E_{li})) + O(pN^{-2}) \right] = \\ &= \Gamma_{l\pm} \left[1 + \beta J_{li} (\mp 1 + \tanh (\beta \Delta E_l)) + O(pN^{-2}) \right], \end{aligned} \quad (\text{S37})$$

where in the last passage we used the fact that $\Delta E_{li} = \Delta E_l + O(\sqrt{p}/N)$. We now perform this substitution in the last addend of Eq. (S24), which yields

$$\begin{aligned} &\frac{\gamma}{2} \sigma_i^+ \sum_{l \neq i} (1 + \sigma_i^z) \Gamma_{l-}^2 \left\{ 1 + \beta J_{li} (1 + \tanh \beta \Delta E_l) - \frac{1}{2} [1 + \beta J_{li} (1 + \tanh \beta \Delta E_l)]^2 - \frac{1}{2} + O(pN^{-2}) \right\} = \\ &= \frac{\gamma}{2} \sigma_i^+ \sum_{l \neq i} (1 + \sigma_i^z) \Gamma_{l-}^2 \left\{ -\frac{1}{2} [\beta J_{li} (1 + \tanh \beta \Delta E_l)]^2 + O(pN^{-2}) \right\} = \frac{\gamma}{2} \sigma_i^+ \sum_{l \neq i} (1 + \sigma_i^z) \Gamma_{l-}^2 \{ O(pN^{-2}) \} = O(pN^{-1}) \end{aligned} \quad (\text{S38})$$

and the same holds for the other term involving Γ_{l+} . Therefore, we can safely neglect these terms in the thermodynamic limit, which produces a considerably simplified form of the dynamical equations

$$\dot{\sigma}_i^{\pm} = \mp i \Omega \sigma_i^z - \frac{\gamma}{2} \sigma_i^{\pm}. \quad (\text{S39})$$

The equations can be further simplified by expressing them in the (x, y, z) basis:

$$\dot{\sigma}_i^z = 2\Omega \sigma_i^y - \gamma \sigma_i^z + \gamma \tanh (\beta \Delta E_i), \quad (\text{S40a})$$

$$\dot{\sigma}_i^y = -2\Omega \sigma_i^z - \frac{\gamma}{2} \sigma_i^y, \quad (\text{S40b})$$

$$\dot{\sigma}_i^x = -\frac{\gamma}{2} \sigma_i^x. \quad (\text{S40c})$$

Interestingly enough, the equation for σ_i^x decouples from the others and one can conveniently restrict to the y and z components only. At this level, it is already possible to appreciate a striking difference with the classical case. Indeed,

in order to describe the state of the system, it is not enough to specify the value of N spins, but N vectors need to be specified. Although it will be proved in the next section that this does not dramatically affect the properties of the stationary state, this may give rise to new intriguing phases of the neural network, where it is possible to appreciate competing effects between coherence and dissipation, i.e. a hallmark of the quantum behavior. In the following dynamical mean field equations are derived for this open quantum system. As the geometry of the model is fully connected, in the following we shall employ a mean-field decoupling on different sites, which should yield exact results in the thermodynamic limit.

Dynamical mean field equations and stationary state equations

Before proceeding, it is useful to generalize the definition of the overlaps (S2) to this case:

$$s_\mu^\alpha = \frac{1}{N} \sum_{i=1}^N \xi_i^{(\mu)} \sigma_i^\alpha \quad \mu = 1, \dots, p; \quad \alpha = x, y, z. \quad (\text{S41})$$

These observables can be thought as the overlap between the μ -th memory and the α component of the spins. The equations for these collective variables read

$$\dot{\mathbf{s}}^z = 2\Omega \mathbf{s}^y + \frac{\gamma}{N} \sum_{i=1}^N \boldsymbol{\xi}_i \tanh(\beta \boldsymbol{\xi}_i \cdot \mathbf{s}^z) - \gamma \mathbf{s}^z, \quad (\text{S42})$$

$$\dot{\mathbf{s}}^y = -2\Omega \mathbf{s}^z - \frac{\gamma}{2} \mathbf{s}^y, \quad (\text{S43})$$

where the vectorial notation now groups the pattern indices, not the positional ones: in other words, these are p -uples of operators $\mathbf{s}^\alpha = (s_1^\alpha, \dots, s_p^\alpha)^\top$ and numbers $\boldsymbol{\xi}_i = (\xi_i^{(1)}, \dots, \xi_i^{(p)})^\top$.

Taking the expectation value $\langle \mathbf{s}^\alpha \rangle = \mathbf{m}^\alpha$, it becomes natural at this point to introduce the mean field approximation, by discarding correlations between the collective variables $\langle m_\mu^\alpha m_\nu^\beta \rangle \rightarrow \langle m_\mu^\alpha \rangle \langle m_\nu^\beta \rangle$. Assuming that the memories $\xi^{(\mu)}$ are quenched identically distributed random variables, these equations can be further simplified using the self-averaging hypothesis: denoting by $\langle\langle \cdot \rangle\rangle$ the average over different realizations of the disorder

$$\langle\langle \cdot \rangle\rangle = \int d\boldsymbol{\xi} (\cdot) P(\boldsymbol{\xi}) \quad (\text{S44})$$

with $P(\boldsymbol{\xi})$ the probability distribution function of a pattern $\boldsymbol{\xi}$, we assume that $\mathbf{m}^\alpha \rightarrow \langle\langle \mathbf{m}^\alpha \rangle\rangle$ for $p \rightarrow \infty$, so that

$$\dot{\mathbf{m}}^z = 2\Omega \mathbf{m}^y + \gamma \langle\langle \boldsymbol{\xi} \tanh(\beta \boldsymbol{\xi} \cdot \mathbf{m}^z) \rangle\rangle - \gamma \mathbf{m}^z, \quad (\text{S45})$$

$$\dot{\mathbf{m}}^y = -2\Omega \mathbf{m}^z - \frac{\gamma}{2} \mathbf{m}^y. \quad (\text{S46})$$

The equations for the stationary state are then straightforwardly obtained setting $\dot{\mathbf{m}}^\alpha = 0$:

$$2\Omega \mathbf{m}^y + \gamma \langle\langle \boldsymbol{\xi} \tanh(\beta \boldsymbol{\xi} \cdot \mathbf{m}^z) \rangle\rangle - \gamma \mathbf{m}^z = 0, \quad (\text{S47})$$

$$2\Omega \mathbf{m}^z + \frac{\gamma}{2} \mathbf{m}^y = 0, \quad (\text{S48})$$

and thus:

$$\frac{8\Omega^2 + \gamma^2}{\gamma^2} \mathbf{m}^z = \langle\langle \boldsymbol{\xi} \tanh(\beta \boldsymbol{\xi} \cdot \mathbf{m}^z) \rangle\rangle. \quad (\text{S49})$$

This equation clearly shows that the role of the coherent driving Ω is qualitatively similar to that played by the temperature in the classical case, i.e. at large enough Ω the non-trivial solutions of the equation disappear, as in the classical case. This also shows that introducing a coherent driving does not change the mean field stationary phase diagram of the Hopfield model, as already shown in [36]. Nevertheless, due to the coupled and non-linear nature of the above equations, new *oscillating* phases, i.e. limit cycles, could appear. In the next section the possible emergence of such solutions is investigated.

To explicitly map out the properties of the model, a specific form for the disorder distribution must be fixed. Our choice, which has already been considered in the literature [19], is:

$$P(\boldsymbol{\xi}) = \prod_{\mu=1}^p p(\xi^{(\mu)}), \quad p(\xi) = \frac{1}{2} \delta(\xi - 1) + \frac{1}{2} \delta(\xi + 1). \quad (\text{S50})$$

The aim in the following is to characterize the phase diagram of this open quantum Hopfield model in the (Ω, β) -plane. For simplicity, we measure all frequencies (and inverse times) in units of γ and effectively set $\gamma = 1$. Some considerations can now be formulated:

1. For both small T and Ω , a slightly-perturbed retrieval phase is expected, i.e. the overlap parameter \mathbf{m}^z has to converge to a value close to $\mathbf{m}^z(t \rightarrow \infty) = (1, 0, \dots, 0)$ (or to one of the others $p-1$ equivalent vectors).
2. For large enough T , a paramagnetic phase is expected, i.e. thermal fluctuations destroy both retrieval and coherence and $\mathbf{m}^z \rightarrow \mathbf{0}$ at infinite time.
3. For small T and large enough Ω , new time-dependent solutions could appear. The appearance of such solutions can be inferred from a high- T expansion arrested at the first non-linear terms, which shows that Eqs. (S46) realize a generalized Lotka-Volterra system, for which the existence of limit-cycles, i.e. periodic time-dependent solutions, is well-known [24]. The role of predator-prey competition (or mutualism) in that ecological system is played here by coherent-thermal competition.

MAPPING OUT THE PHASE DIAGRAM: STABILITY ANALYSIS OF THE STATIONARY STATE SOLUTIONS

For the specific choice we made for the distribution of the patterns $\boldsymbol{\xi}$, the equations of motion for $m_\mu^{z/y}$ can be expressed as

$$\dot{m}_\mu^z = 2\Omega m_\mu^y - m_\mu^z + 2^{-p} \sum_{\{\boldsymbol{\xi}\}} \xi^{(\mu)} \tanh[\beta \boldsymbol{\xi} \cdot \mathbf{m}^z], \quad (\text{S51})$$

$$\dot{m}_\mu^y = -2\Omega m_\mu^z - \frac{1}{2} m_\mu^y, \quad (\text{S52})$$

where the sum runs over all possible choices of p -vectors $\boldsymbol{\xi}^\top = (\xi^{(1)}, \dots, \xi^{(p)})$ with $\xi^{(\mu)}$ a classical Ising variable which can only take the values ± 1 .

These equations display a large class of symmetries:

- (i) *variable permutation*: $(m_\mu^z, m_\mu^y) \leftrightarrow (m_\nu^z, m_\nu^y)$;
- (ii) *single mode inversion*: $(m_\mu^z, m_\mu^y) \rightarrow (-m_\mu^z, -m_\mu^y)$.

Because of the presence of these symmetries, the dynamics displays a set of invariant subspaces:

- (a) $(m_\mu^z, m_\mu^y) = (0, 0)$;
- (b) $(m_\mu^z, m_\mu^y) = (m_\nu^z, m_\nu^y)$;
- (c) $(m_\mu^z, m_\mu^y) = (-m_\nu^z, -m_\nu^y)$.

In particular, in subspace (a) the μ -th mode can be effectively discarded and the equations reduce to the $p-1$ case. In other words, the p -memories case always includes all the p' -memories cases with $p' < p$ as special instances.

Stability analysis of the paramagnetic solution

We provide here a very brief summary of the stability analysis for the paramagnetic solution $(m_\mu^z, m_\mu^y) = (0, 0) \forall i$. We thus take a small perturbation from the fixed point $m_\mu^\alpha = 0 + \delta m_\mu^\alpha$ and expand the equations to first order:

$$\delta \dot{m}_\mu^z = 2\Omega \delta m_\mu^y - \delta m_\mu^z + 2^{-p} \beta \sum_{\{\boldsymbol{\xi}\}} \xi^{(\mu)} \boldsymbol{\xi} \cdot \delta \mathbf{m}^z, \quad (\text{S53a})$$

$$\delta \dot{m}_\mu^y = -2\Omega \delta m_\mu^z - \frac{1}{2} \delta m_\mu^y. \quad (\text{S53b})$$

The sum over configurations annihilates all terms $\xi^{(\mu)}\xi^{(\nu)}\delta m_\nu^z$ with $i \neq j$. This ensures that the stability equations for different modes decouple:

$$\delta \dot{m}_\mu^z = 2\Omega \delta m_\mu^y - \delta m_\mu^z + \beta \delta m_\mu^z, \quad (\text{S54a})$$

$$\delta \dot{m}_\mu^y = -2\Omega \delta m_\mu^z - \frac{1}{2} \delta m_\mu^y. \quad (\text{S54b})$$

The stability matrix can thus be reduced to a 2×2 -block structure, with the μ -th block reading

$$S_\mu = \begin{pmatrix} \beta - 1 & 2\Omega \\ -2\Omega & -\frac{1}{2} \end{pmatrix}, \quad (\text{S55})$$

with eigenvalues

$$\begin{aligned} \lambda_\pm &= \frac{1}{2} \left[\beta - \frac{3}{2} \pm \sqrt{\left(\beta - \frac{3}{2}\right)^2 + 2(\beta - \beta_c)} \right] = \\ &= \frac{1}{2} \left[\beta - \frac{3}{2} \pm \sqrt{\left(\beta - \frac{1}{2}\right)^2 - 16\Omega^2} \right] \end{aligned} \quad (\text{S56})$$

with the shorthand $\beta_c = 1 + 8\Omega^2$. We can thus distinguish the following regimes:

- (I) $\beta > \beta_c = 8\Omega^2 + 1$ implies that the eigenvalues are real and have different signs, i.e., we have a saddle point in the origin (it is unstable with a single stable direction);
- (II) $\{\beta < \beta_c\} \cap \{\beta > 3/2\} \cap \{\beta > 4\Omega + 1/2\}$: the eigenvalues are real and positive, i.e., the fixed point is unstable;
- (III) $\{\beta < \beta_c\} \cap \{\beta > 3/2\} \cap \{\beta < 4\Omega + 1/2\}$: the eigenvalues are complex conjugates with positive real part. The fixed point is unstable and spiraling;
- (IV) $\{\beta < \beta_c\} \cap \{\beta < 3/2\} \cap \{|\beta - 1/2| < 4\Omega\}$: the eigenvalues are complex conjugates with negative real part. The fixed point is stable and spiraling.
- (V) $\{\beta < \beta_c\} \cap \{\beta < 3/2\} \cap \{|\beta - 1/2| > 4\Omega\}$: the eigenvalues are real and negative. The fixed point is stable.

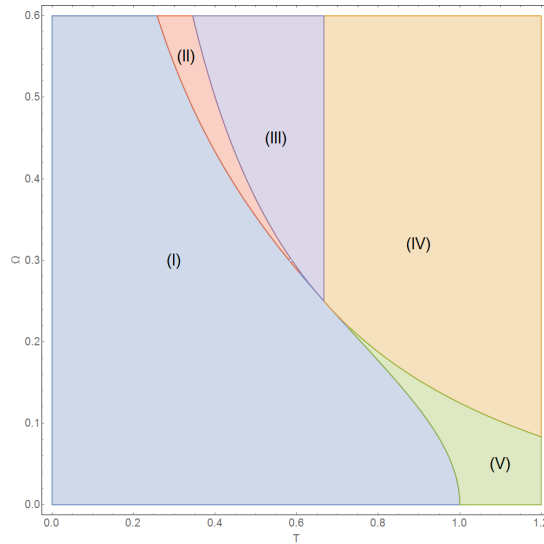


FIG. S1. Stability regimes in the $T - \Omega$ plane.

Appearance and stability of the ferromagnetic solutions

We now turn to the presence of non-vanishing stationary solutions of the form

$$m_\mu^\alpha = \overline{m}^\alpha \delta_{\mu\nu} \quad (\text{S57})$$

for some fixed $\nu \in \{1, \dots, p\}$. As done in the main text, we shall refer to these solutions as *ferromagnetic*, as opposed to the vanishing *paramagnetic* one discussed above. These ferromagnetic solutions satisfy the stationary equation

$$\beta_c \overline{m}^z = \tanh(\beta \overline{m}^z) \quad (\text{S58})$$

and can only exist if the \tanh function has a non-trivial intersection with the line expressed in the l.h.s. apart from the origin. This only occurs for $\beta > \beta_c$. The stability can be analyzed along the same lines used for the vanishing solution: without loss of generality, due to the symmetry under exchange, we can limit ourselves to studying the case where the only non-vanishing component is the first one. We consider small perturbations

$$m_1^\alpha = \overline{m}^\alpha + \delta m_1^\alpha \quad (\text{S59})$$

$$m_\mu^\alpha = \delta m_\mu^\alpha \quad \forall \mu > 1 \quad (\text{S60})$$

and expand to first-order the equations of motion (S51), (S52), which again decouple to

$$\delta \dot{m}_\mu^z = 2\Omega \delta m_\mu^y - \delta m_\mu^z + \frac{\beta}{\cosh^2(\beta \overline{m}^z)} \delta m_\mu^z, \quad (\text{S61a})$$

$$\delta \dot{m}_\mu^y = -2\Omega \delta m_\mu^z - \frac{1}{2} \delta m_\mu^y. \quad (\text{S61b})$$

for all $\mu \in \{1, \dots, p\}$. Note that these equations are equivalent to the ones found for the stability of the paramagnetic solution up to the substitution

$$\beta \rightarrow \beta' = \frac{\beta}{\cosh^2(\beta \overline{m}^z)}, \quad (\text{S62})$$

which defines an effective inverse temperature β' which depends upon β and, through \overline{m}^z , upon Ω .

The stability analysis can now borrow from the one performed for the paramagnetic solution: for $\Omega < 1/4$ the latter is stable for $\beta < \beta_c$. Analogously, the ferromagnetic solutions will be stable for $\beta' < \beta_c$, with $\beta' = \beta_c$ marking the boundary where the stability changes. This boundary satisfies by definition

$$\beta_c = \beta' = \frac{\beta}{\cosh^2(\beta \overline{m}^z)} = \beta (1 - \tanh^2(\beta \overline{m}^z)), \quad (\text{S63})$$

whence we read off

$$\beta \overline{m}^z = \operatorname{arctanh} \sqrt{1 - \frac{\beta_c}{\beta}}. \quad (\text{S64})$$

By substitution in Eq. (S58) we thus find

$$\frac{\beta_c}{\beta} \operatorname{arctanh} \sqrt{1 - \frac{\beta_c}{\beta}} = \sqrt{1 - \frac{\beta_c}{\beta}}. \quad (\text{S65})$$

As one would expect, this equation is only well-defined for $\beta \geq \beta_c$, since $\beta = \beta_c$ marks the disappearance of the ferromagnetic solutions. Setting $\beta_c/\beta = \tau$ we have to solve

$$f(\tau) \equiv \tau \operatorname{arctanh} \sqrt{1 - \tau} - \sqrt{1 - \tau} = 0, \quad (\text{S66})$$

which is trivially satisfied for $\tau = 1$ (i.e., on the line $\beta = \beta_c$). However, $f'(\tau) = \operatorname{arctanh} \sqrt{1 - \tau} > 0$ for $\tau \in [0, 1)$, implying that f is strictly increasing on this interval and thus $\tau = 1$ is the only physical point where $f \equiv 0$. In other words, the ferromagnetic solutions are always stable for $\Omega < 1/4$ and $\beta > \beta_c$.

We now turn to the complementary case $\Omega \geq 1/4$, where the stability boundary is instead $\beta' = 3/2$. Correspondingly, from Eq. (S62) we derive

$$\frac{3}{2} = \beta' = \frac{\beta}{\cosh^2(\beta \bar{m}^z)} = \beta (1 - \tanh^2(\beta \bar{m}^z)), \quad (\text{S67})$$

implying

$$\beta \bar{m}^z = \operatorname{arctanh} \sqrt{1 - \frac{3}{2\beta}}. \quad (\text{S68})$$

Substituting in Eq. (S58) yields now

$$\frac{\beta_c}{\beta} \operatorname{arctanh} \sqrt{1 - \frac{3}{2\beta}} = \sqrt{1 - \frac{3}{2\beta}}. \quad (\text{S69})$$

Recalling our previous definition $\beta_c = 8\Omega^2 + 1$, we find now that the stability boundary for $\Omega \geq 1/4$ is

$$\Omega^2 = \frac{1}{8} \left[\frac{\sqrt{\beta(\beta - \frac{3}{2})}}{\operatorname{arctanh} \sqrt{1 - \frac{3}{2\beta}}} - 1 \right] = B(\beta), \quad (\text{S70})$$

with $\Omega^2 < B(\beta)$ being the stable regime and $\Omega^2 > B(\beta)$ the unstable one. We also remark that on this boundary

$$\beta_c = \beta \frac{\sqrt{1 - \frac{3}{2\beta}}}{\operatorname{arctanh} \sqrt{1 - \frac{3}{2\beta}}} < \beta, \quad (\text{S71})$$

which implies that, as expected, the stability line always lies at *lower* temperatures than the critical line $\beta = \beta_c$.

Role of the effective temperature

We now employ the concept of effective temperature β' defined above to give a qualitative characterization of what we can expect to observe in a multiple-memory scenario. We thus take the case of $p-1$ memories with a finite overlap $(m_\mu^z)^2 + (m_\nu^z)^2 \neq 0$ and a single mode m_p^α which is slightly perturbed away from its origin $m_p^\alpha = \delta m_p^\alpha \ll 1$. We define for brevity $\boldsymbol{\xi}' = (\xi^{(1)}, \dots, \xi^{(p-1)})$ and $\mathbf{m}'^\alpha = (\mathbf{m}_1^\alpha, \dots, \mathbf{m}_{p-1}^\alpha)$. To leading order, the dynamical equations for the last mode read

$$\delta \dot{m}_p^z = 2\Omega \delta m_p^y - \delta m_p^z + 2^{1-p} \beta \left(\sum_{\{\boldsymbol{\xi}'\}} \frac{1}{\cosh^2(\beta \boldsymbol{\xi}' \cdot \mathbf{m}'^z)} \right) \delta m_p^z, \quad (\text{S72a})$$

$$\delta \dot{m}_p^y = -2\Omega \delta m_p^z - \frac{1}{2} \delta m_p^y. \quad (\text{S72b})$$

The stability matrix can therefore be again expressed as

$$S = \begin{pmatrix} \beta' - 1 & 2\Omega \\ -2\Omega & -\frac{1}{2} \end{pmatrix} \quad \text{with} \quad \beta' = 2^{1-p} \beta \left(\sum_{\{\boldsymbol{\xi}'\}} \frac{1}{\cosh^2(\beta \boldsymbol{\xi}' \cdot \mathbf{m}'^z)} \right) \leq \beta. \quad (\text{S73})$$

In other words, every finite overlap tends to increase the temperature of the ones close to the paramagnetic point $(0,0)$. In particular, this provides a qualitative explanation of the fact that numerically — except when starting very close to a symmetric subspace where two or more modes are equal in modulus (i.e., $m_\mu^\alpha \approx \pm m_\nu^\alpha$) — we never see more than two overlaps displaying ample oscillations: at every time, the presence of one of the two modes with a large amplitude stabilizes the others around zero. Similarly, when we observe a single mode with a large oscillation amplitude, the other modes remain very close to 0 except around the nodes of the first curve, where indeed their effective temperature decreases, making the origin unstable for them.

LIMIT CYCLE PHASE: EXACT RESULTS AND NUMERICAL SOLUTION

Representation of the $p = 1$ case in terms of a Liénard equation

Once specialized to a single-memory case, the equations of motion read

$$\dot{m}^z = 2\Omega m^y - m^z + \tanh[\beta m^z], \quad (\text{S74a})$$

$$\dot{m}^y = -2\Omega m^z - \frac{1}{2}m^y. \quad (\text{S74b})$$

From the first equation we can extract

$$m^y = \frac{1}{2\Omega} [\dot{m}^z + m^z - \tanh[\beta m^z]], \quad (\text{S75})$$

which we can substitute in the second. Now, deriving with respect to time the first equation we get

$$\begin{aligned} \ddot{m}^z &= 2\Omega \dot{m}^y - \dot{m}^z + \frac{\beta}{\cosh^2 \beta m^z} \dot{m}^z = \\ &= -4\Omega^2 m^z - \frac{1}{2} (\dot{m}^z + m^z - \tanh[\beta m^z]) - \dot{m}^z + \frac{\beta}{\cosh^2 \beta m^z} \dot{m}^z = \\ &= \frac{1}{2} [\tanh[\beta m^z] - (8\Omega^2 + 1)m^z] + \left[\frac{\beta}{\cosh^2 \beta m^z} - \frac{3}{2} \right] \dot{m}^z, \end{aligned} \quad (\text{S76})$$

which can be rewritten as $\ddot{m}^z + F'(m^z)\dot{m}^z + G'(m^z) = 0$, with

$$F'(m^z) = \frac{3}{2} - \frac{\beta}{\cosh^2 \beta m^z} \quad \text{and} \quad G'(m^z) = \frac{1}{2} [(8\Omega^2 + 1)m^z - \tanh[\beta m^z]]. \quad (\text{S77})$$

This equation is in Liénard form [26]. The corresponding Liénard theorem states that if

- (L1) F' and G' are continuous functions of their arguments;
- (L2) F and G' are odd functions and $G'(x) > 0$ for $x > 0$;
- (L3) F has only one positive, simple root a (such that $F(a) = 0$);
- (L4) $F'(0) < 0$;
- (L5) $F'(x) \geq 0$ for $x > a$ and $F(x) \rightarrow +\infty$ when $x \rightarrow +\infty$,

then the system exhibits a single limit cycle around the origin and the limit cycle is stable.

We now have to check in what parameter regime the hypotheses are simultaneously satisfied. (L1) is trivial. For (L2) we choose

$$F(m^z) = \int_0^{m^z} dy F'(y) = \frac{3}{2}m^z - \tanh(\beta m^z), \quad (\text{S78})$$

while $G' > 0$ for positive values of the argument only when $\beta < \beta_c = 8\Omega^2 + 1$. This constitutes our first constraint. (L3) only holds when $\beta > 3/2$ and thus provides a second constraint. (L4) is also verified for $\beta > 3/2$. Finally, the second part of (L5) – i.e., $F(x \rightarrow \infty) \rightarrow \infty$ – is easily verified; we now check that for $\beta > 3/2$ the first part holds as well: to do this, we notice that $F'(m^z)$ has only a single zero for $m^z > 0$, since $1/\cosh^2(x)$ is a monotonically decreasing function for $x > 0$. Let us call this point z ; note that this constitutes an extremum for F . Now, the asymptotic behavior of F for $m^z \rightarrow 0^+$ is given by $F(m^z) \approx (3/2 - \beta)m^z + o(m^z)$, implying that there must be a neighborhood of 0 such that all the points in this set that are > 0 yield negative values of F . On the other hand, $F(x \rightarrow +\infty) \rightarrow +\infty$ and F is continuous, so it must take a minimum for some $m^z > 0$. This must coincide with the extremum z . Hence, $F(z) < 0$ and $F'(m^z) > 0$ for at least some $m^z > z$, but F' is continuous and there is no $m^z > z$ in which it vanishes, so F' must be positive $\forall m^z > z$. In particular, the single root of F must appear after z by the intermediate-value (or Darboux) property and the uniqueness of the root, concluding our check.

To summarize, the hypotheses of Liénard theorem are satisfied by our equations in the regime $\{\beta < \beta_c\} \cap \{\beta > 3/2\}$. Here we are guaranteed that only one limit cycle exists and it is stable.

Representation of the $p = 1$ case in terms of a single $N/2$ -spin

We show here that the dynamical equations can be effectively reduced to describe the evolution of a single global spin. We thus define the operators

$$S^z = \sum_i \xi_i \sigma_i^z, \quad S^y = \sum_i \xi_i \sigma_i^y \quad \text{and} \quad S^x = \sum_i \sigma_i^x. \quad (\text{S79})$$

We now show that these three quantities satisfy the canonical $SU(2)$ algebra commutation relations (up to a trivial multiplying factor)

$$[S^\alpha, S^\beta] = 2i\epsilon_{\alpha\beta\gamma} S^\gamma. \quad (\text{S80})$$

We start with

$$[S^x, S^y] = \sum_{jl} \xi_l [\sigma_j^x, \sigma_l^y] = \sum_{jl} \xi_l \delta_{jl} 2i\sigma_j^z = 2i \sum_j \xi_j \sigma_j^z = 2iS^z. \quad (\text{S81})$$

Secondly, we have

$$[S^y, S^z] = \sum_{jl} \xi_j \xi_l [\sigma_j^y, \sigma_l^z] = \sum_{jl} \xi_j \xi_l \delta_{jl} 2i\sigma_j^x = 2i \sum_j \underbrace{(\xi_j)^2}_{=1} \sigma_j^x = 2iS^x \quad (\text{S82})$$

and finally

$$[S^z, S^x] = \sum_{jl} \xi_j [\sigma_j^z, \sigma_l^x] = \sum_{jl} \xi_j \delta_{jl} 2i\sigma_j^y = 2i \sum_j \xi_j \sigma_j^y = 2iS^y. \quad (\text{S83})$$

Dividing by N one obtains the corresponding intensive observables $s^\alpha = S^\alpha/N$ (note that s^x here differs from the one defined above by not being multiplied by the pattern ξ). These quantities obey $[s^\alpha, s^\beta] = 2i\epsilon_{\alpha\beta\gamma} s^\gamma/N \rightarrow 0$ in the thermodynamic limit and can be therefore regarded as semiclassical variables which evolve according to the equations

$$\dot{s}^z = 2\Omega s^y + \frac{\gamma}{N} \sum_{i=1}^N \xi_i \tanh(\beta \xi_i s^z) - \gamma s^z, \quad (\text{S84})$$

$$\dot{s}^y = -2\Omega s^z - \frac{\gamma}{2} s^y, \quad (\text{S85})$$

$$\dot{s}^x = -\frac{\gamma}{2} s^x. \quad (\text{S86})$$

These equations can be considered exact up to finite size corrections scaling as $1/N$. If $N \gg 1$ one can furthermore approximate the non-linear term with the law of large numbers and thus recover (the $p = 1$ instance of) Eqs. (S45) and (S46). The one-memory case can thus be interpreted as a large classical spin precessing around the x axis with frequency 2Ω and undergoing an additional non-unitary and non-linear dynamics which invariably reduces the long-time evolution to the $y-z$ plane.

The 2-memories case

In the 2-memories case, the non-linear system consists of four equations. Specializing Eqs. (S51) and (S52) for $p = 2$ we get

$$\dot{m}_1^z = 2\Omega m_1^y + \frac{1}{2} [\tanh(\beta(m_1^z + m_2^z)) + \tanh(\beta(m_1^z - m_2^z))] - m_1^z, \quad (\text{S87})$$

$$\dot{m}_2^z = 2\Omega m_2^y + \frac{1}{2} [\tanh(\beta(m_1^z + m_2^z)) + \tanh(\beta(m_2^z - m_1^z))] - m_2^z, \quad (\text{S88})$$

$$\dot{m}_1^y = -2\Omega m_1^z - \frac{1}{2} m_1^y, \quad (\text{S89})$$

$$\dot{m}_2^y = -2\Omega m_2^z - \frac{1}{2} m_2^y. \quad (\text{S90})$$

The solutions of these equations can be investigated as a function of the 4 initial conditions $m_\mu^\alpha(0)$. The qualitative stationary behavior should be independent of the specific choice of these values, apart from the special hyperplanes (of zero-measure in this 4-dimensional space) given by the invariant subspaces identified in the previous sections. In Fig. S2 some examples are reported which display the typical dynamical behavior in the three different phases (paramagnetic, retrieval and limit cycles) discussed in the main text.

A general feature is that once a small coherent term is added, both components of the order parameters m^z, m^y are non-zero, and there is a deviation from perfect retrieval, also at zero temperature. For small T and large enough Ω limit cycles appear. Also in this case perfect retrieval is not possible. A closer look of this regime shows that the m_1^z and m_2^z (and their respective y counterparts) oscillate in quadrature, i.e. maximum overlap with one memory is obtained close to where zero overlap with the other is achieved. Also in this case a comparison with the Lotka-Volterra competitive system helps, indeed in that case the interpretation is straightforward: once the number of preys is large, predators have a considerable amount of food and thus their number increases, eventually making the number of preys dwindle, which in turn will cause starvation among the predators and reduce their population, and so on. This mechanism leads to periodic oscillations in the preys/predators number with a relative phase of approximately $\pi/2$. This ecological comparison suggests that in some sense the different memories stored in the network are competing with each other qualitatively in the same way (at least in this simple 2-memories case). This behavior is highlighted also in Fig. S2.

Decoupling of the equations in the 2-memories case

The case $p = 2$ is particularly interesting, since it can be reduced to a couple of independent one-memory ($p = 1$) systems: the equations for the four overlaps m_μ^α read in this case

$$\dot{m}_1^z = 2\Omega m_1^y - m_1^z + \frac{1}{2} [\tanh(\beta(m_1^z + m_2^z)) + \tanh(\beta(m_1^z - m_2^z))], \quad (\text{S91a})$$

$$\dot{m}_1^y = -2\Omega m_1^z - \frac{1}{2} m_1^y, \quad (\text{S91b})$$

$$\dot{m}_2^z = 2\Omega m_2^y - m_2^z + \frac{1}{2} [\tanh(\beta(m_1^z + m_2^z)) - \tanh(\beta(m_1^z - m_2^z))], \quad (\text{S91c})$$

$$\dot{m}_2^y = -2\Omega m_2^z - \frac{1}{2} m_2^y. \quad (\text{S91d})$$

Defining now $M^\alpha = m_1^\alpha + m_2^\alpha$ and $m^\alpha = m_1^\alpha - m_2^\alpha$ we can separate the equations into

$$\dot{M}^z = 2\Omega M^y - M^z + \tanh(\beta M^z), \quad (\text{S92a})$$

$$\dot{M}^y = -2\Omega M^z - \frac{1}{2} M^y \quad (\text{S92b})$$

and

$$\dot{m}^z = 2\Omega m^y - m^z + \tanh(\beta m^z), \quad (\text{S93a})$$

$$\dot{m}^y = -2\Omega m^z - \frac{1}{2} m^y. \quad (\text{S93b})$$

Each pair constitutes now an independent system equivalent to a $p = 1$ problem. In particular, this implies that the only ferromagnetic solutions (m_1^z, m_2^z) one can find in this case have one of the forms $(\bar{m}, 0)$, $(0, \bar{m})$, (\bar{m}, \bar{m}) or $(\bar{m}, -\bar{m})$, with the former two being stable in the retrieval regime and the latter two always unstable.

Furthermore, due to the uniqueness of the attractive limit cycle, in the LC phase the sum and difference undergo equal oscillations up to a phase shift θ which is determined by the respective initial conditions. Tuning this phase shift corresponds to varying the relative amplitude of oscillation of the overlaps m_1 and m_2 between the limiting cases $\theta = 0$ ($m_2 \equiv 0$) and $\theta = \pi$ ($m_1 \equiv 0$). In Fig. S3 two examples are reported to highlight this relation. The two overlaps $m_{1/2}$ generically oscillate close to quadrature (i.e., the extremal points of m_1^z occur close to the nodes of m_2^z and vice versa). An exception can be found in the coexistence region of retrieval points and limit cycles, which allows, say, the difference to reach a non-trivial stationary value while the sum ends on a limit cycle and oscillates indefinitely. In this case, the two overlaps oscillate in-phase (or in antiphase if the roles of sum and difference are exchanged) up to an additive constant.

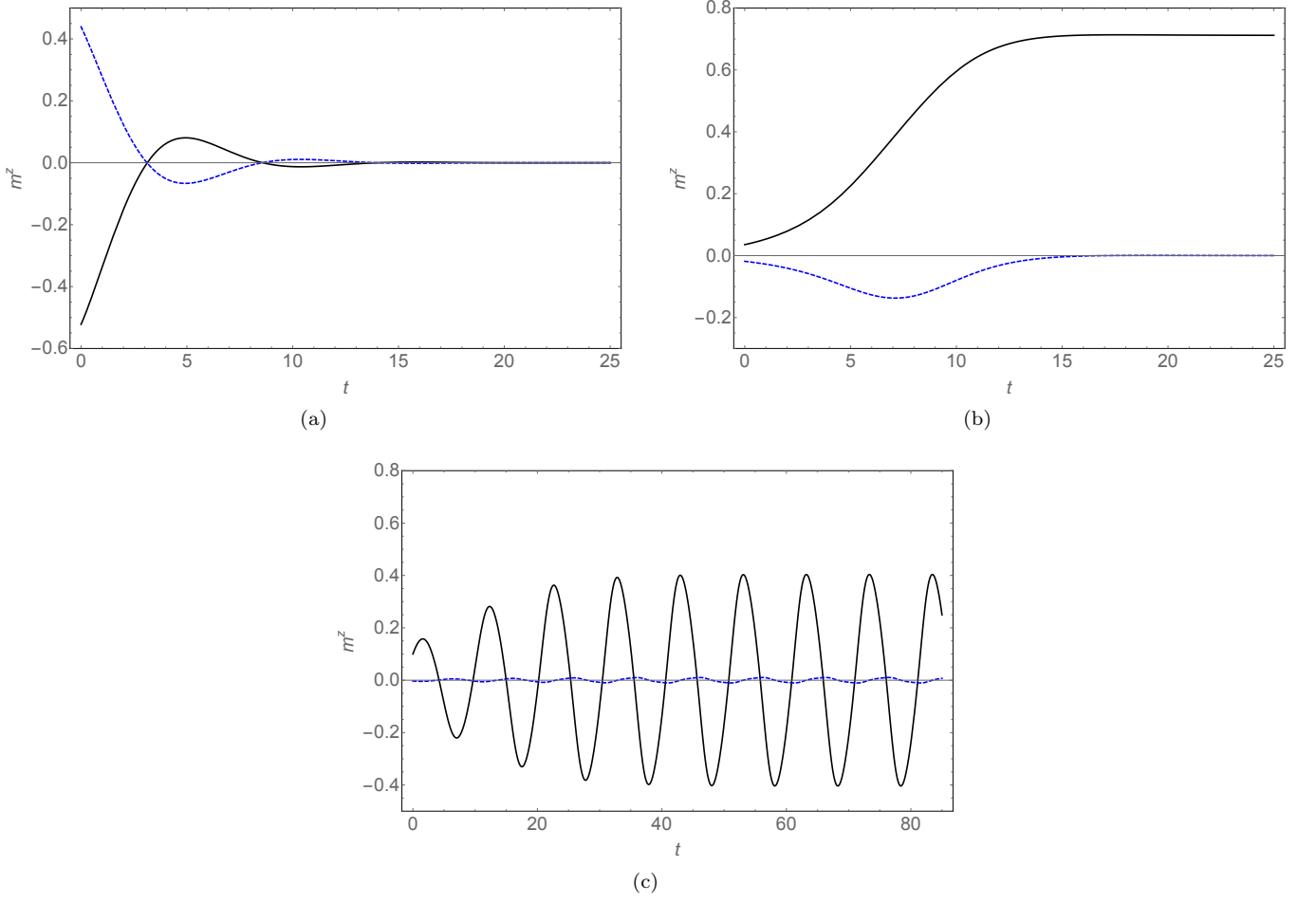


FIG. S2. Plots of the dynamical evolution of the overlaps m_1^z (black solid line), m_2^z (blue dashed line) as functions of times for three choices of the parameters: (a) $\Omega = 0.3$ and $T = 1.2$ is well inside the paramagnetic phase and the overlaps vanish in the long-time limit. (b) $\Omega = 0.1$ and $T = 0.7$ identifies instead a point within the retrieval phase and one overlap reaches a finite stationary value. (c) for $\Omega = 0.4$ and $T = 0.6$ the system lies in the limit-cycle phase and the overlaps oscillate periodically. In particular, starting from an initial condition in which one overlap dominates while the other is much smaller the evolution leads to the former oscillating with a large amplitude, while the latter remains confined to a neighborhood of the origin. This property seems to hold for higher values of p as well.

The 3-memories case

Despite the number of equations grows only linearly in the number of memories, the number of terms in each equation grows exponentially, limiting the brute force approach to the problem. We briefly discuss here the behavior of the $p = 3$ case, as the simplest example in which the equations do not decouple. The 6 dynamical equations, reported for completeness, read

$$\dot{m}_z^1 = 2\Omega m_y^1 + \frac{1}{4} [\tanh(\beta(m_z^1 + m_z^2 + m_z^3)) + \tanh(\beta(m_z^1 - m_z^2 + m_z^3)) + \tanh(\beta(m_z^1 + m_z^2 - m_z^3)) + \tanh(\beta(m_z^1 - m_z^2 - m_z^3))] - m_z^1, \quad (\text{S94})$$

$$+ \tanh(\beta(m_z^1 + m_z^2 - m_z^3)) + \tanh(\beta(m_z^1 - m_z^2 - m_z^3))] - m_z^1, \quad (\text{S95})$$

$$\dot{m}_z^2 = 2\Omega m_y^2 + \frac{1}{4} [\tanh(\beta(m_z^1 + m_z^2 + m_z^3)) + \tanh(\beta(m_z^2 - m_z^1 + m_z^3)) + \tanh(\beta(m_z^2 + m_z^1 - m_z^3)) + \tanh(\beta(m_z^2 - m_z^1 - m_z^3))] - m_z^2, \quad (\text{S96})$$

$$+ \tanh(\beta(m_z^2 + m_z^1 - m_z^3)) + \tanh(\beta(m_z^2 - m_z^1 - m_z^3))] - m_z^2, \quad (\text{S97})$$

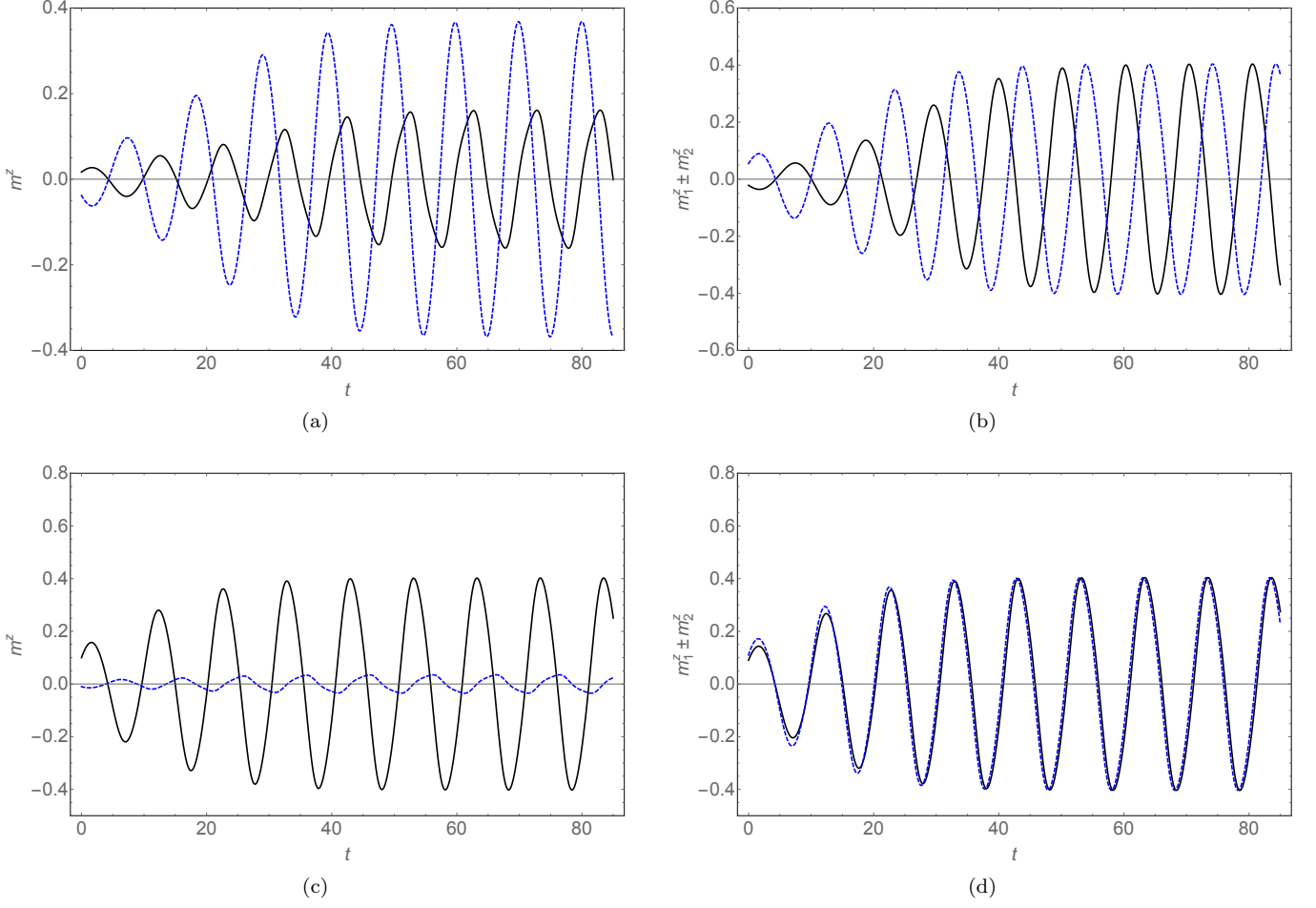


FIG. S3. (a) Evolution of the overlaps m_1^z (black solid line) and m_2^z (blue dashed line) in the limit cycle phase ($\Omega = 0.4$ and $T = 0.6$) for a random choice of initial conditions. (b) Plot of the sum $m_1^z + m_2^z$ (black solid line) and difference $m_1^z - m_2^z$ (blue dashed line) of the overlaps as functions of time for the same initial condition and parameters employed for (a). At long times the sum and difference undergo equal oscillations up to a phase shift. This shift depends on the initial conditions and is reflected in the overall amplitude of the oscillations experienced by m_1^z and m_2^z . Panels (c,d) differ from (a,b) solely by the initial condition and are reported for comparison.

$$\dot{m}_z^3 = 2\Omega m_y^3 + \frac{1}{4} \left[\tanh(\beta(m_z^1 + m_z^2 + m_z^3)) + \tanh(\beta(m_z^3 - m_z^1 + m_z^2)) + \right. \quad (\text{S98})$$

$$\left. + \tanh(\beta(m_z^3 + m_z^1 - m_z^2)) + \tanh(\beta(m_z^3 - m_z^1 - m_z^2)) \right] - m_z^3, \quad (\text{S99})$$

$$\dot{m}_y^1 = -2\Omega m_z^1 - \frac{1}{2} m_y^1, \quad (\text{S100})$$

$$\dot{m}_y^2 = -2\Omega m_z^2 - \frac{1}{2} m_y^2, \quad (\text{S101})$$

$$\dot{m}_y^3 = -2\Omega m_z^3 - \frac{1}{2} m_y^3. \quad (\text{S102})$$

The relevant static solutions are again the paramagnetic and retrieval points. In the limit cycle phase, for random initial conditions the limit cycle phase always displays two oscillating overlaps while the third decays to zero, reducing the problem effectively to $p = 2$. Albeit it is not a formal proof, the mechanism seems related to the effective heating exerted by the two larger modes on the third, smaller one – see the “effective temperature” (S73) – which shifts it in its paramagnetic phase. By applying the considerations made in the previous section, we therefore find that by starting with a single dominant overlap and two suppressed ones the system will end up oscillating almost entirely on the first mode, whereas the other two will remain confined around zero, as shown in Fig. (S4). Numerical solutions of the equations up to $p = 12$ show the same qualitative behavior: only two modes survive in the long-time limit,

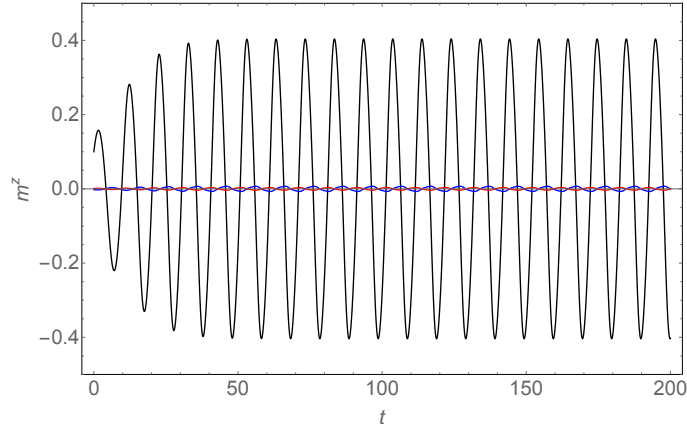


FIG. S4. Limit cycle for $p = 3$, $\Omega = 0.4$ and $T = 0.6$. The three curves correspond to m_1^z (black), m_2^z (blue) and m_3^z (red), with an initial condition chosen such that $m_1^z \gg m_2^z, m_3^z$ and $m_i^y = 0 \forall i$. As reported in the main text, this choice ensures that at long times only m^1 will display non-negligible oscillations, while the remaining two overlaps can be neglected with good approximation.

although the duration of the transient seems to increase with the number of patterns p .

Bounds to the appearance of limit cycles

We consider here how to determine the presence and amplitude of limit cycles, and more specifically to set some bounds for them. We start with the one-memory case; out of symmetry considerations, we choose a family of ellipses in the $m^z - m^y$ plane which map onto themselves under the \mathbb{Z}_2 transformation $m^\alpha \rightarrow -m^\alpha$. These are parametrized by

$$(m^z)^2 + \lambda^2 (m^y)^2 + 2\lambda \cos \theta (m^z m^y) = r^2 \quad (\text{S103})$$

for some $\lambda \geq 0$, $\theta \in [0, \pi]$ and $r \geq 0$. For $\lambda = 1$, $\theta = \pi/2$ this describes the circle of radius r centered in the origin. At fixed λ and θ , the ellipses obtained for different r do not intersect and cover the entire plane. In the following, we shall treat λ and θ as parameters and r^2 as a dynamical variable defined in terms of m^z and m^y . Its time derivative reads

$$\begin{aligned} \partial_t r^2 &= 2 [m^z \dot{m}^z + \lambda^2 m^y \dot{m}^y + \lambda \cos \theta (m^z \dot{m}^y + m^y \dot{m}^z)] = \\ &= (m^y)^2 [4\Omega \lambda \cos \theta - \lambda^2] - m^y [4\Omega m^z (1 - \lambda^2) - 3\lambda \cos \theta m^z + 2\lambda \cos \theta \tanh(\beta m^z)] + \\ &- 2 [(m^z)^2 - m^z \tanh(\beta m^z) + 2\Omega \lambda \cos \theta (m^z)^2]. \end{aligned} \quad (\text{S104})$$

Note that any point in the plane lies on a uniquely defined ellipse, implying that $\partial_t r^2 < 0$ means that the flux from that point enters the ellipse, whereas it exits it for $\partial_t r^2 > 0$. Furthermore, if this derivative never changes sign then there can be no limit cycles, since a periodic solution for m^z and m^y would determine a periodic time dependence of r^2 as well, which is impossible if its derivative never changes sign. We notice now that the equation $\partial_t r^2 = 0$ is quadratic in m^y ; to assess the presence of real solutions we can thus study the discriminant

$$\begin{aligned} \Delta &= [4\Omega m^z (1 - \lambda^2) - 3\lambda \cos \theta m^z + 2\lambda \cos \theta \tanh(\beta m^z)]^2 + \\ &+ 8 (4\Omega \lambda \cos \theta - \lambda^2) [(m^z)^2 - m^z \tanh(\beta m^z) + 2\Omega \lambda \cos \theta (m^z)^2] = \\ &= A(m^z)^2 + B m^z \tanh(\beta m^z) + C \tanh^2(\beta m^z), \end{aligned} \quad (\text{S105})$$

with

$$\begin{aligned} A &= [4\Omega(1 - \lambda^2) - 3\lambda \cos \theta]^2 + 8\lambda(4\Omega \cos \theta - \lambda)(1 + 2\Omega \lambda \cos \theta) \\ B &= 4\lambda \cos \theta [4\Omega(1 - \lambda^2) - 3\lambda \cos \theta] - 8(4\Omega \lambda \cos \theta - \lambda^2) \\ C &= 4\lambda^2 \cos^2 \theta. \end{aligned} \quad (\text{S106})$$

The discriminant can be recast as

$$\Delta = A \left(m^z + \frac{\tanh \beta m^z}{2A} (B + \sqrt{B^2 - 4AC}) \right) \left(m^z + \frac{\tanh \beta m^z}{2A} (B - \sqrt{B^2 - 4AC}) \right). \quad (\text{S107})$$

We distinguish two regimes: (I) if $A < 0$ then

$$\Delta = -|A| \left(m^z - \frac{\tanh \beta m^z}{2|A|} \underbrace{(B + \sqrt{B^2 + 4|A|C})}_{>=0} \right) \left(m^z + \frac{\tanh \beta m^z}{2|A|} \underbrace{(\sqrt{B^2 + 4|A|C} - B)}_{>=0} \right) \quad (\text{S108})$$

and the discriminant can only change sign if

$$\frac{\beta}{2|A|} (B + \sqrt{B^2 + 4|A|C}) > 1. \quad (\text{S109})$$

If for fixed physical parameters Ω and β

$$\mathcal{S} = \{A < 0\} \cap \left\{ \frac{\beta}{2A} (B + \sqrt{B^2 - 4AC}) < 1 \right\} \neq \emptyset \quad (\text{S110})$$

then for any choice of $(\lambda, \theta) \in \mathcal{S}$ the discriminant is *always* negative and one can conclude the absence of limit cycles and stationary points besides the origin. The second regime (II) is $A \geq 0$, in which case the discriminant is negative for small values of m^z if

$$\frac{\beta}{2A} (-B + \sqrt{B^2 - 4AC}) > 1. \quad (\text{S111})$$

If this is the case, one can identify a threshold value of m_i^z below which the discriminant remains negative. All ellipses confined within are therefore crossed in one direction only.

For the multiple-memories case ($p > 1$), one can take an ellipsoid defined as

$$|\mathbf{m}^z|^2 + \lambda^2 |\mathbf{m}^y|^2 + 2\lambda \cos \theta (\mathbf{m}^z \cdot \mathbf{m}^y) = r^2, \quad (\text{S112})$$

such that $\partial_t r^2 = a |\mathbf{m}^y|^2 - \mathbf{b} \cdot \mathbf{m}^y + c$ with

$$a = 4\Omega\lambda \cos \theta - \lambda^2, \quad (\text{S113a})$$

$$\mathbf{b} = \left[4\Omega \mathbf{m}^z (1 - \lambda^2) - 3\lambda \cos \theta \mathbf{m}^z + (2\lambda \cos \theta) 2^{-p} \sum_{\{\xi\}} \xi \tanh(\beta \xi \cdot \mathbf{m}^z) \right] \quad (\text{S113b})$$

$$c = -2 \left[|\mathbf{m}^z|^2 - 2^{-p} \sum_{\{\xi\}} \xi \cdot \mathbf{m}^z \tanh(\beta \xi \cdot \mathbf{m}^z) + 2\Omega\lambda \cos \theta |\mathbf{m}^z|^2 \right]. \quad (\text{S113c})$$

The extremal condition for having solutions to $\partial_t r^2 = 0$ is now

$$\begin{aligned} 0 = \Delta &= |\mathbf{b}|^2 - 4ac = \\ &= A |\mathbf{m}^z|^2 + B 2^{-p} \sum_{\{\xi\}} \xi \cdot \mathbf{m}^z \tanh(\beta \xi \cdot \mathbf{m}^z) + C \left[2^{-p} \sum_{\{\xi\}} \xi \tanh(\beta \xi \cdot \mathbf{m}^z) \right]^2 \end{aligned} \quad (\text{S114})$$

with A, B, C as in Eq. (S106). Analogously to the one-memory case, the discriminant can be recast as

$$\begin{aligned} \Delta &= A \left(\mathbf{m}^z + 2^{-p} \sum_{\{\xi\}} \xi \frac{\tanh \beta \xi \cdot \mathbf{m}^z}{2A} (B + \sqrt{B^2 - 4AC}) \right) \cdot \\ &\quad \cdot \left(\mathbf{m}^z + 2^{-p} \sum_{\{\xi'\}} \xi' \frac{\tanh \beta \xi' \cdot \mathbf{m}^z}{2A} (B - \sqrt{B^2 - 4AC}) \right). \end{aligned} \quad (\text{S115})$$

Again, if for some choice of the parameters Ω and β we find $\mathcal{S} \neq \emptyset$, then a family of ellipsoids can be identified such that all dynamical trajectories enter them, and thus no limit cycles can appear, nor stationary solutions of any kind apart from the origin.

Finally, note that for the circles, $\lambda = 1$ and $\cos \theta = 0$, we have $A = -B = -8$ and $C = 0$, implying

$$\Delta = -8 \left[|\mathbf{m}^z|^2 - 2^{-p} \sum_{\{\boldsymbol{\xi}\}} \boldsymbol{\xi} \cdot \mathbf{m}^z \tanh \beta \boldsymbol{\xi} \cdot \mathbf{m}^z \right]. \quad (\text{S116})$$

Now, using the fact that $x \tanh(\beta x) \leq \beta x^2$ we find

$$\Delta \leq -8 \left[|\mathbf{m}^z|^2 - 2^{-p} \beta \sum_{\{\boldsymbol{\xi}\}} (\boldsymbol{\xi} \cdot \mathbf{m}^z)^2 \right] = -8 |\mathbf{m}^z|^2 (1 - \beta), \quad (\text{S117})$$

where the last equality comes from the fact that

$$\sum_{\{\boldsymbol{\xi}\}} \xi_\mu \xi_\nu = 2^p \delta_{\mu\nu}. \quad (\text{S118})$$

This indicates that for $\beta < 1$ no limit cycles can appear and the origin is the only stationary point. Furthermore, consistently with the stability analysis, it is attractive as it can be easily verified that the trajectories actually *enter* the circles.

For the circles, we can also verify that all trajectories enter the unit sphere in $2p$ dimensions for *any* choice of the parameters Ω and β : fixing $\lambda = 1$ and $\cos \theta = 0$ implies $a = -1$, $\mathbf{b} = 0$ and

$$c = -2 \left[|\mathbf{m}^z|^2 - 2^{-p} \sum_{\{\boldsymbol{\xi}\}} \boldsymbol{\xi} \cdot \mathbf{m}^z \tanh(\beta \boldsymbol{\xi} \cdot \mathbf{m}^z) \right]. \quad (\text{S119})$$

We now substitute $|\mathbf{m}^y|^2 = r^2 - |\mathbf{m}^z|^2$ into $\partial_t r^2$ to find

$$\begin{aligned} \partial_t r^2 &= -r^2 - |\mathbf{m}^z|^2 + 2^{1-p} \sum_{\{\boldsymbol{\xi}\}} \boldsymbol{\xi} \cdot \mathbf{m}^z \tanh(\beta \boldsymbol{\xi} \cdot \mathbf{m}^z) = \\ &= -r^2 - |\mathbf{m}^z|^2 + 2^{1-p} \sum_{\{\boldsymbol{\xi}\}} |\boldsymbol{\xi} \cdot \mathbf{m}^z \tanh(\beta \boldsymbol{\xi} \cdot \mathbf{m}^z)| = \\ &= -r^2 - |\mathbf{m}^z|^2 + 2^{1-p} \sum_{\{\boldsymbol{\xi}\}} |\boldsymbol{\xi} \cdot \mathbf{m}^z| |\tanh(\beta \boldsymbol{\xi} \cdot \mathbf{m}^z)| \leq \\ &\leq -r^2 - |\mathbf{m}^z|^2 + 2^{1-p} \sum_{\{\boldsymbol{\xi}\}} |\boldsymbol{\xi} \cdot \mathbf{m}^z|. \end{aligned} \quad (\text{S120})$$

The next step is to show that

$$2^{-p} \sum_{\{\boldsymbol{\xi}\}} |\boldsymbol{\xi} \cdot \mathbf{m}^z| \leq |\mathbf{m}^z| \quad (\text{S121})$$

This is easily achieved via Cauchy-Schwarz inequality, since the l.h.s. is the average $\langle |\boldsymbol{\xi} \cdot \mathbf{m}^z| \rangle$ and we know that for any random variable $\langle A \rangle \leq \sqrt{\langle A^2 \rangle}$, implying in our case

$$2^{-p} \sum_{\{\boldsymbol{\xi}\}} |\boldsymbol{\xi} \cdot \mathbf{m}^z| \leq \sqrt{2^{-p} \sum_{\{\boldsymbol{\xi}\}} |\boldsymbol{\xi} \cdot \mathbf{m}^z|^2} = \sqrt{|\mathbf{m}^z|^2} = |\mathbf{m}^z|, \quad (\text{S122})$$

where we have used the identity (S118). Consequently,

$$\partial_t r^2 \leq -r^2 - |\mathbf{m}^z|^2 + 2 |\mathbf{m}^z| = -(|\mathbf{m}^z| - 1)^2 + 1 - r^2 \leq 1 - r^2 \leq 0 \quad (\text{S123})$$

if $r^2 \geq 1$.

- [2] C. M. Bishop, *Machine Learning* **128** (2006).
- [3] V. Mnih, K. Kavukcuoglu, D. Silver, A. A. Rusu, J. Veness, M. G. Bellemare, A. Graves, M. Riedmiller, A. K. Fidjeland, G. Ostrovski, *et al.*, *Nature* **518**, 529 (2015).
- [4] D. Silver, A. Huang, C. J. Maddison, A. Guez, L. Sifre, G. Van Den Driessche, J. Schrittwieser, I. Antonoglou, V. Panneershelvam, M. Lanctot, *et al.*, *Nature* **529**, 484 (2016).
- [5] G. E. Hinton and R. R. Salakhutdinov, *Science* **313**, 504 (2006).
- [6] P. W. Shor, *SIAM Review* **41**, 303 (1999).
- [7] L. K. Grover, *Phys. Rev. Lett.* **79**, 325 (1997).
- [8] T. Monz, D. Nigg, E. A. Martinez, M. F. Brandl, P. Schindler, R. Rines, S. X. Wang, I. L. Chuang, and R. Blatt, *Science* **351**, 1068 (2016).
- [9] V. S. Denchev, S. Boixo, S. V. Isakov, N. Ding, R. Babbush, V. Smelyanskiy, J. Martinis, and H. Neven, *Phys. Rev. X* **6**, 031015 (2016).
- [10] S. Mandrà, Z. Zhu, and H. G. Katzgraber, arXiv preprint arXiv:1606.07146 (2016).
- [11] H. Nishimori, arXiv preprint arXiv:1609.03785 (2016).
- [12] J. Biamonte, P. Wittek, N. Pancotti, P. Rebentrost, N. Wiebe, and S. Lloyd, arXiv preprint arXiv:1611.09347 (2016).
- [13] D. Ventura and T. Martinez, *Information Sciences* **124**, 273 (2000).
- [14] A. A. Ezhov and D. Ventura, in *Future directions for intelligent systems and information sciences* (Springer, 2000) pp. 213–235.
- [15] S. Gupta and R. Zia, *Journal of Computer and System Sciences* **63**, 355 (2001).
- [16] M. Schuld, I. Sinayskiy, and F. Petruccione, *Quantum Information Processing* **13**, 2567 (2014).
- [17] H.-P. Breuer and F. Petruccione, *The theory of open quantum systems* (Oxford University Press on Demand, 2002).
- [18] J. J. Hopfield, *Proceedings of the National Academy of Sciences* **79**, 2554 (1982).
- [19] D. J. Amit, H. Gutfreund, and H. Sompolinsky, *Phys. Rev. A* **32**, 1007 (1985).
- [20] D. J. Amit, H. Gutfreund, and H. Sompolinsky, *Phys. Rev. Lett.* **55**, 1530 (1985).
- [21] D. J. Amit, H. Gutfreund, and H. Sompolinsky, *Annals of Physics* **173**, 30 (1987).
- [22] see supplemental material, .
- [23] M. Mézard, G. Parisi, and M.-A. Virasoro, *Spin glass theory and beyond*. (World Scientific Publishing Co., Inc., Pergamon Press, 1990).
- [24] Y. Takeuchi, *Global dynamical properties of Lotka-Volterra systems* (World Scientific, 1996).
- [25] A. M. Lyapunov, *International Journal of Control* **55**, 531 (1992).
- [26] A. Palit and D. Prasad Datta, ArXiv e-prints (2010), arXiv:1003.0114 [math.CA].
- [27] M. Hirsch, S. Smale, and R. Devaney, *Differential Equations, Dynamical Systems, and an Introduction to Chaos*, Pure and Applied Mathematics; A Series of Monographs and Text (Elsevier Science, 2003).
- [28] C.-K. Chan, T. E. Lee, and S. Gopalakrishnan, *Phys. Rev. A* **91**, 051601 (2015).
- [29] A. C. C. Coolen and T. W. Ruijgrok, *Phys. Rev. A* **38**, 4253 (1988).
- [30] M. Evans, *Journal of Physics A: Mathematical and General* **22**, 2103 (1989).
- [31] B. Baumgartner and H. Narnhofer, *J. Phys. A* **41**, 395303 (2008).
- [32] V. V. Albert and L. Jiang, *Phys. Rev. A* **89**, 022118 (2014).
- [33] V. V. Albert, B. Bradlyn, M. Fraas, and L. Jiang, *Phys. Rev. X* **6**, 041031 (2016).
- [34] K. Macieszczak, M. Guta, I. Lesanovsky, and J. P. Garrahan, *Phys. Rev. Lett.* **116**, 240404 (2016).
- [35] P. Zanardi and L. Campos Venuti, *Phys. Rev. Lett.* **113**, 240406 (2014).
- [36] H. Nishimori and Y. Nonomura, *Journal of the Physical Society of Japan* **65**, 3780 (1996).